

Study of Block Diagonalization Precoding and Power Allocation for Multiple-Antenna Systems with Coarsely Quantized Signals

Silvio F. B. Pinto and Rodrigo C. de Lamare

Abstract

In this work, we present block diagonalization and power allocation algorithms for large-scale multiple-antenna systems with coarsely quantized signals. In particular, we develop Coarse Quantization-Aware Block Diagonalization (CQA-BD) and Coarse Quantization-Aware Regularized Block Diagonalization (CQA-RBD) precoding algorithms that employ the Bussgang decomposition and can mitigate the effects of low-resolution signals and interference. Moreover, we also devise the Coarse Quantization-Aware Most Advantageous Allocation Strategy (CQA-MAAS) power allocation algorithm to improve the sum rate of precoders that operate with low-resolution signals. An analysis of the sum-rate performance is carried out along with computational complexity and power consumption studies of the proposed and existing techniques. Simulation results illustrate the performance of the proposed CQA-BD and CQA-RBD precoding algorithms, and the proposed CQA-MAAS power allocation strategy against existing approaches.

Index Terms

Quantization, consumption, power allocation, block diagonalization, Bussgang's theorem.

I. INTRODUCTION

In the last decade, research efforts in wireless communications have shown a great deal of progress in massive multiple-input multiple-output (MIMO) systems. In particular, massive MIMO systems employ base-stations (BS) with a large number of antennas that can serve dozens of users. However, the increasing numbers of antennas at the BS results in higher costs in terms of equipment and power consumption. Therefore, the design of effective and economical massive MIMO systems to equip networks with satisfactory coverage and power consumption will require low-cost components and more energy-efficient algorithms [1], [2], [3], [4], [5], [6]. In fact, approaches to energy-efficient design of precoding and detection algorithms have relied on signal quantization with few bits followed by cost-effective strategies such as receive filters, detectors and estimators that can compensate for the loss due to coarse quantization [8], [9], [10], [11], [13], [21]. Each transmit antenna at the BS is connected to a radio-frequency (RF) chain, which includes digital-to-analog converters (DACs), low noise amplifier (LNA), mixers, oscillators,

automatic gain control (AGC) and filters. Among these components, the power consumption of DACs dominates the total power of the RF chain. In particular, low-resolution DACs are important to reduce the power consumption associated with the transmitter. The power consumption can be substantially reduced when the number of bits used by DACs is reduced because it grows exponentially with the number of quantization bits.

A. Prior and Related Work

Despite the progress in 1-bit quantization [13], [21] with the aim of reducing power consumption in the large number of DACs used in massive MIMO systems, the achievable sum rates remain relatively low, which makes higher resolution quantizers with $b = 2, 3, 4, 5, 6$ bits attractive for the design of linear precoders and receivers. In this context, Busgang's theorem [57] let us express Gaussian precoded signals that have been quantized as a linear function of the quantized input and a distortion term which has no correlation with the input [8], [9], [10]. This approach makes possible the computation of sum-rates of Gaussian signals [12].

In particular, block diagonalization (BD)-type precoding methods [23], [25], [26], [27], [24], [28] are known as linear transmit approaches for multiuser MIMO (MU-MIMO) systems based on singular value decompositions (SVD), which provide excellent achievable sum-rates in the case of significant levels of multi-user interference and multiple-antenna users. BD precoding is motivated by its enhanced sum-rate performance as compared to standard linear zero forcing (ZF) and minimum mean-square error (MMSE) precoders and its suitability for use with power allocation due to the available power loading matrix with the singular values that avoids an extra SVD. However, BD has not been thoroughly investigated with coarsely quantized signals so far. In addition, existing linear ZF and MMSE precoding techniques that employ 1-bit quantization in massive MU-MIMO systems often present relatively poor performance and significant losses relative to full-resolution precoders. Furthermore, precoding techniques in MU-MIMO systems can greatly benefit from power allocation strategies such as waterfilling. Specifically, power allocation can greatly enhance the sum-rate and error rate performance by employing higher power levels for channels with larger gains and lower power levels for poor channels. Previous works in this area have considered iterative waterfilling techniques [54], practical algorithms [55] and specific strategies for BD precoders [56] even though there has been no power allocation strategy that takes into account coarse quantization so far, which could enhance the performance of precoders with low-resolution signals.

B. Contributions

In this work, we present BD and power allocation algorithms for large-scale MU-MIMO systems with coarsely quantized signals [30]. Specifically, we develop Coarse Quantization-Aware Block Diagonalization (CQA-BD) and Coarse Quantization-Aware Regularized Block Diagonalization (CQA-RBD) precoding

algorithms that employ the Bussgang decomposition and can mitigate the effects of low-resolution signals and interference. Moreover, we also devise a Coarse Quantization-Aware Most Advantageous Allocation Strategy (CQA-MAAS) power allocation algorithm, which aims to perform the most advantageous power allocation in the presence of coarsely-quantized signals and imperfect channel knowledge to maximize the sum-rate performance. An analysis of the sum-rate is developed along with a computational complexity study of the proposed and existing techniques. Numerical results illustrate the excellent performance of the proposed CQA-BD and CQA-RBD precoding and CQA-MAAS power allocation algorithms against existing approaches. The main contributions of this work can be summarized as:

- We present the CQA-BD and CQA-RBD precoding algorithms for large-scale MU-MIMO systems with coarsely quantized signals.
- We develop the CQA-MAAS power allocation algorithm for linearly-precoded MU-MIMO systems.
- An analysis of the sum-rate is devised along with studies of computational complexity and power consumption.
- A comparative study of the proposed and existing precoding and power allocation.

This paper is structured as follows. Section II describes the system model and background for understanding the proposed CQA-BD class algorithms. Section III presents the proposed CQA-BD type algorithms. Section IV introduces the proposed CQA-MAAS power allocation algorithm, whereas Section V details how precoding and power allocation work together. Section VI analyzes the sum-rate performance, the computational complexity and the power consumption of the proposed algorithms. Section VII presents and discusses numerical results whereas the conclusions are drawn in Section VIII.

Notation: the superscript H denotes the Hermitian transposition, the superscript $*$ stands for the complex conjugate, $\mathbb{E}[\cdot]$ expresses the expectation operator, \mathbf{I}_M stands for the $M \times M$ identity matrix, and $\mathbf{0}_M$ represents a $M \times 1$ vector whose elements are all zero.

II. SYSTEM MODEL AND BACKGROUND

Let us consider the broadcast channel (BC) of a MU-MIMO system with a BS containing N_b antennas, which sends radio frequency (RF) signals to users equipped with a total of $N_u = \sum_{j=1}^K N_j$ receive antennas, where $N_j \geq 1$ denotes the number of receive antennas of the j th user U_j , $j = 1, \dots, K$, as outlined in Fig. 1.

We can model the input-output relation of the BC as

$$\mathbf{y} = \mathbf{H} \mathbf{s}_q + \mathbf{n}, \quad (1)$$

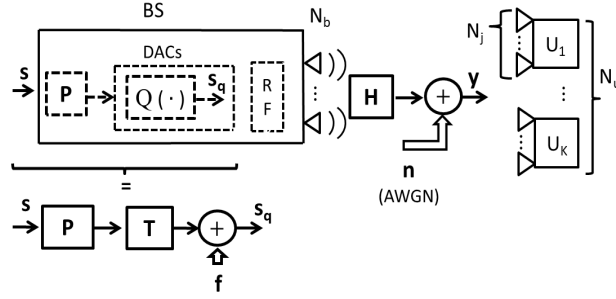


Fig. 1. Outline of a quantized massive MU-MIMO downlink system. Upper diagram: some simplified parts of BS. Lower diagram: Bussgang's theorem applied to the detached part of interest.

where $\mathbf{y} \in \mathbb{C}^{N_u}$ contains the signals received by all users and $\mathbf{H} \in \mathbb{C}^{N_u \times N_b}$ stands for the matrix which models the assumed broadcast channel that is assumed known to the BS. The entries of \mathbf{H} are considered independent circularly-symmetrical complex Gaussian random variables $[\mathbf{H}]_{u,b} \in \mathbb{CN}(0, 1)$, $u = 1, \dots, N_u$ and $b = 1, \dots, N_b$. The noise vector $\mathbf{n} \in \mathbb{C}^{N_u}$ is characterized by its independent and identically distributed (i.i.d.) circularly-symmetric complex Gaussian entries $n_u \in \mathbb{CN}(0, N_0)$. We consider that the noise variance is known at the BS and so is the sampling rate of DACs at BS and ADCs at user equipments. In order to provide a better understanding, we include here a short overview of Bussgang's theorem, which allows to deal successfully with nonlinearities like the distortion generated by DACs.

Theorem 1. *Given two Gaussian signals, the cross-correlation function taken after one of them has undergone nonlinear amplitude distortion is identical, except for a scaling factor, to the cross-correlation function taken before the distortion [12], [57]. Specifically, according to Bussgang's theorem, for a pair of zero-mean jointly complex Gaussian random variables $y_m \sim \mathbb{CN}(0, \sigma_{y_m}^2)$ and $y_n \sim \mathbb{CN}(0, \sigma_{y_n}^2)$, and for the output r_m of some scalar-valued nonlinear function $r_m = f(y_m)$, where $f(\cdot) : \mathbb{C} \rightarrow \mathbb{C}$ expresses an element-wise function application, it holds that*

$$\mathbb{E}_{r_m, y_n} [r_m y_n^*] = g_m \mathbb{E}_{y_m, y_n} [y_m y_n^*] \quad (2)$$

in which

$$g_m = \frac{1}{\sigma_{y_m}^2} \mathbb{E}_{y_m} [f(y_m) y_m^*] \quad (3)$$

Let us consider now that the previously mentioned nonlinear function $f(\cdot)$ can be applied element-wise to a zero-mean complex Gaussian random vector $\mathbf{y} = [y_1, y_2, \dots, y_M] \sim \mathbb{CN}(\mathbf{0}_{M \times 1}, \mathbf{C}_y)$, resulting in a vector \mathbf{f} , i.e., $\mathbf{r} = f(\mathbf{y})$. It follows from (2) that

$$\mathbf{C}_{\mathbf{r}\mathbf{y}} = \mathbf{G} \mathbf{C}_y \quad (4)$$

where

$$\mathbf{G} = \text{diag} \left([g_1, g_2, \dots, g_M]^T \right) \quad (5)$$

represents a diagonal $M \times M$ matrix whose m th diagonal entry is computed as in (3). Busgang's theorem can be used to decompose the output of a nonlinear device as a linear function of the input \mathbf{y} plus a distortion $\mathbf{d} \in \mathbb{C}^M$ that is uncorrelated (but not independent) with the input as [12]:

$$\mathbf{r} = \mathbf{G}\mathbf{y} + \mathbf{d} \quad (6)$$

The referred uncorrelation can be viewed as follows:

$$\begin{aligned} \mathbb{E} [\mathbf{d}\mathbf{y}^H] &= \mathbb{E} [(\mathbf{r} - \mathbf{G}\mathbf{y})\mathbf{y}^H] \\ &= \mathbf{C}_{\mathbf{r}\mathbf{y}} - \mathbf{G} \mathbf{C}_{\mathbf{y}} = \mathbf{0}_{M \times M} \end{aligned} \quad (7)$$

where we made use of (4).

Thus, following the lower part of Fig.1, the quantization $\mathbf{Q}(\cdot)$ of a precoded symbol vector $\mathbf{P}\mathbf{s}$, where $\mathbf{P} \in \mathbb{C}^{N_b \times N_u}$ is a precoding matrix and $\mathbf{s} \sim \mathbb{CN}(\mathbf{0}_{N_u \times 1}, \mathbf{I}_{N_u})$ is the symbol vector, can be expressed by the quantized vector given by

$$\mathbf{s}_q = \mathbf{Q}(\mathbf{P}\mathbf{s}) = \mathbf{T}\mathbf{P}\mathbf{s} + \mathbf{f}, \quad (8)$$

where the distortion term \mathbf{f} , also known as quantization error, and the symbol \mathbf{s} vectors are uncorrelated as shown in (7). Although this term is not Gaussian, in Subsection V-B, we will see that for approximations of achievable sum-rates involving N_b and N_u sufficiently large, it can be approximated as Gaussian noise, i.e., $\mathbf{f} \in \mathbb{C}^{N_b}$, whose entries $f_b \in \mathbb{CN}(0, \sigma_d^2)$. For the general case, $\mathbf{T} \in \mathbb{R}^{N_b \times N_b}$ is the diagonal matrix expressed [8] by

$$\begin{aligned} \mathbf{T}_{n,n} &= \frac{\alpha\gamma}{\sqrt{\pi}} \text{diag}(\mathbf{P}\mathbf{P}^H)^{-1/2} \cdot \\ &\quad \sum_{l=1}^{J-1} \exp\left(-\gamma^2 \left(l - \frac{J}{2}\right)^2 \text{diag}(\mathbf{P}\mathbf{P}^H)^{-1}\right) \end{aligned} \quad (9)$$

where $n = 1 \dots N_b$, and J and γ stand for the number of levels and the step size of the quantizer, respectively. The scalar factor $\alpha \in \mathbb{R}$, which will be detailed in Subsection V-B, has the purpose of satisfying the average power constraint

$$\mathbb{E} [\|\mathbf{P}\mathbf{s}\|_2^2] \leq P \quad (10)$$

where the transmit power is given by

$$P = \text{SNR} N_0, \quad (11)$$

where SNR is the signal-to-noise ratio.

III. PROPOSED CQA-BD AND CQA-RBD PRECODING ALGORITHMS

In this section, we present the proposed coarse-quantization aware (CQA) precoding techniques. In particular, the proposed precoders encompass the CQA-BD and its regularized version CQA-RBD. The derivation of the CQA-BD and CQA-RBD precoding algorithms exploits the knowledge of the channel matrix that contains the channel coefficients of the links between the BS and the users along with SVD operations. In particular, BD type precoding techniques [23], [25], [27] are SVD-based transmit processing algorithms which are performed in two stages. The precoder computed in the first stage suppresses (BD) or attempts to obtain a trade-off between MUI and noise (RBD). Afterwards, parallel or near-parallel single user (SU)-MIMO are calculated. The proposed CQA-BD and CQA-RBD algorithms can be obtained from the minimization of globally optimum cost functions, which lead to unique solutions to these optimization problems.

Both CQA-BD and CQA-RBD algorithms compute a precoding matrix \mathbf{P}_j for the j th user that can be expressed as the product

$$\mathbf{P}_j = \mathbf{P}_j^c \mathbf{P}_j^d \quad (12)$$

where $\mathbf{P}_j^c \in \mathbb{C}^{N_b \times L_j}$ and $\mathbf{P}_j^d \in \mathbb{C}^{L_j \times N_j}$. The parameter L_j depends on which precoding algorithm is chosen, namely, the CQA-BD or CQA-RBD techniques.

We can express the combined channel matrix \mathbf{H} and the resulting precoding matrix \mathbf{P} as follows:

$$\mathbf{H} = [\mathbf{H}_1^T \mathbf{H}_2^T \cdots \mathbf{H}_K^T]^T \in \mathbb{C}^{N_u \times N_b} \quad (13)$$

$$\mathbf{P} = [\mathbf{P}_1 \mathbf{P}_2 \cdots \mathbf{P}_K] \in \mathbb{C}^{N_b \times N_u} \quad (14)$$

where $\mathbf{H}_j \in \mathbb{C}^{N_j \times N_b}$ is the channel matrix of the j th user. The matrix $\mathbf{P}_j \in \mathbb{C}^{N_b \times N_j}$ represents the precoding matrix of the j th user.

A. CQA-BD Precoder

In the proposed CQA-BD precoding algorithm, the first factor in (12) is given by

$$\mathbf{P}_j^{c(\text{CQA-BD})} = \overline{\mathbf{W}}_j^{(0)} \quad (15)$$

where $\overline{\mathbf{W}}_j^{(0)}$ is obtained by the SVD [27] of (13), in which the channel matrix of the j th user has been removed, i.e.:

$$\begin{aligned}\overline{\mathbf{H}}_j &= [\mathbf{H}_1^T \cdots \mathbf{H}_{j-1}^T \mathbf{H}_{j+1}^T \cdots \mathbf{H}_K^T]^T \in \mathbb{C}^{\overline{N}_j \times N_b} \\ &= \overline{\mathbf{U}}_j \overline{\Phi}_j \overline{\mathbf{W}}_j^H = \overline{\mathbf{U}}_j \overline{\Phi}_j \left[\overline{\mathbf{W}}_j^{(1)} \overline{\mathbf{W}}_j^{(0)} \right]^H\end{aligned}\quad (16)$$

where $\overline{N}_j = N_u - N_j$. The matrix $\overline{\mathbf{W}}_j^{(0)} \in \mathbb{C}^{N_b \times (N_b - \overline{L}_j)}$, where \overline{L}_j is the rank of $\overline{\mathbf{H}}_j$, uses the last $N_b - \overline{L}_j$ singular vectors.

The second precoder of CQA-BD in (12) is obtained by SVD of the effective channel matrix for the j th user \mathbf{H}_{e_j} and employs a power loading matrix as follows:

$$\mathbf{P}_j^{d(\text{CQA-BD})} = \mathbf{W}_j^{(1)} \left(\Omega_j^{(\text{CQA-BD})} \right)^{\frac{1}{2}} \quad (17)$$

where the power loading matrix $\Omega_j^{(\text{CQA-BD})}$ requires a power allocation algorithm and the matrix $\mathbf{W}_j^{(1)}$ incorporates the first $\Lambda_e = \text{rank}(\mathbf{H}_{e_j})$ singular vectors obtained by the decomposition of \mathbf{H}_{e_j} , as follows:

$$\begin{aligned}\mathbf{H}_{e_j} &= \mathbf{H}_j \mathbf{P}_j^c = \mathbf{U}_j \Phi_j \mathbf{W}_j^H \\ &= \mathbf{U}_j \begin{bmatrix} \Phi_j & 0 \\ 0 & 0 \end{bmatrix} \left[\mathbf{W}_j^{(1)} \quad \mathbf{W}_j^{(0)} \right]^H\end{aligned}\quad (18)$$

B. CQA-RBD Precoder

In the case of the proposed CQA-RBD precoding algorithm, the global optimization that leads to its design is given by

$$\mathbf{P}_j^{c(\text{CQA-RBD})} = \min_{\mathbf{P}_j^c} \mathbb{E} \left[\|\overline{\mathbf{H}}_k \mathbf{P}_j^c\|^2 + \frac{\|\mathbf{n}_j\|^2}{P} \right], \quad (19)$$

The first precoder in (12) is given [25], [27] by

$$\mathbf{P}_j^{c(\text{CQA-RBD})} = \overline{\mathbf{W}}_j \left(\overline{\Phi}_j^T \overline{\Phi}_j + \chi \mathbf{I}_{N_b} \right)^{-1/2} \quad (20)$$

where $\chi = \frac{N_u \sigma_n^2}{P}$ is the regularization factor required by the CQA-RBD algorithm and P is the average transmit power.

The second precoder of CQA-RBD in (12) is obtained by SVD of the effective channel matrix for the j th user \mathbf{H}_{e_j} and power loading, respectively as follows:

$$\mathbf{P}_j^{d(\text{CQA-RBD})} = \mathbf{W}_j \left(\Omega_j^{(\text{CQA-RBD})} \right)^{\frac{1}{2}} \quad (21)$$

where the matrix $\mathbf{W}_j^{(1)}$ incorporates the early $\Lambda_e = \text{rank}(\mathbf{H}_{e_j})$ singular vectors obtained by the decomposition of \mathbf{H}_{e_j} , as follows:

$$\begin{aligned}\mathbf{H}_{e_j} &= \mathbf{H}_j \mathbf{P}_j^c = \mathbf{U}_j \mathbf{\Phi}_j \mathbf{W}_j^H \\ &= \mathbf{U}_j \begin{bmatrix} \mathbf{\Phi}_j & 0 \\ 0 & 0 \end{bmatrix} \begin{bmatrix} \mathbf{W}_j^{(1)} & \mathbf{W}_j^{(0)} \end{bmatrix}^H\end{aligned}\quad (22)$$

The power loading matrix per user $\mathbf{\Omega}_j^{(CQA-RBD)}$ can be obtained by a procedure like water filling (WF) [29] power allocation and will be initialized with equal power allocation.

With Bussgang's decomposition, the transmit processing equivalence $\mathbf{Q}(\mathbf{P}_s) = \mathbf{T}\mathbf{P}_s + \mathbf{f}$ and the assumption in (9), we obtain the following transmit processing matrix:

$$\mathbf{T}_{n,n} = \delta \mathbf{I}_{N_b \times N_b}, \quad (23)$$

where the scalar factor is described by

$$\delta = \alpha \gamma \sqrt{\frac{N_b}{\pi P}} \sum_{l=1}^{J-1} \exp\left(-\frac{N_b \gamma^2}{P} \left(1 - \frac{J}{2}\right)^2\right) \quad (24)$$

which concentrates all process of quantization on the scalar δ in (23) and is used to compute the sum-rates at the receiver. The loss of achievable sum-rates for a fixed SNR due to the coarse quantization and a fixed realization of the channel are compensated for by $\mathbf{T}_{n,n}$ and δ . The steps needed to compute CQA-BD and CQA-RBD are summarized in Algorithm 1. Extensions to other precoders and/or beamforming strategies [33], [31], [32], [34], [35], [36], [37], [38], [40], [41], [39], [47], [43], [42], [44], [45], [46], [48], [49], [50] are possible. Moreover, detection and parameter estimation strategies can also be considered for future work [61], [62], [63], [64], [65], [66], [67], [68], [69], [60], [70]

C. Precoding and Power Allocation

Here, we detail how the proposed CQA-BD and CQA-RBD precoding and CQA-MAAS power allocation algorithms are carried out prior to data transmission.

Let us consider the precoding and power allocation using the CQA-BD precoder given by

$$\begin{aligned}\mathbf{P}_j^{c(CQA-BD)} &= \mathbf{P}_j^c \mathbf{P}_j^d \\ &= \overline{\mathbf{W}}_j^{(0)} \mathbf{W}_j^{(1)} \left(\mathbf{\Omega}_j^{(CQA-BD)}\right)^{\frac{1}{2}}\end{aligned}\quad (25)$$

where the power loading matrix $\mathbf{\Omega}_j^{(CQA-BD)}$ is computed according to the CQA-MAAS power allocation detailed in Section IV. In particular, the CQA-BD precoder (or CQA-RBD precoder) is computed first with

Algorithm 1 Proposed CQA-BD and CQA-RBD precoders

$$\alpha = \left(2N_b \gamma^2 \left(\left(\frac{J-1}{2} \right)^2 - 2 \sum_{l=1}^{J-1} \left(1 - \frac{J}{2} \right) \Xi \left(\sqrt{2N_b \gamma^2} \left(1 - \frac{J}{2} \right) \right) \right) \right)^{-1/2} \quad (71)$$

$$\delta = \alpha \gamma \sqrt{\frac{N_b}{\pi P}} \sum_{l=1}^{J-1} \exp \left(-\frac{N_b \gamma^2}{P} \left(1 - \frac{J}{2} \right)^2 \right) \quad (24)$$

Require:

$$\mathbf{H} = \left[\mathbf{H}_1^T \mathbf{H}_2^T \cdots \mathbf{H}_K^T \right]^T \in \mathbb{C}^{N_u \times N_b} \quad (13)$$

1: **for** $j = 1 : K$ **do**

$$2: \quad \bar{\mathbf{H}}_j = \left[\mathbf{H}_1^T \cdots \mathbf{H}_{j-1}^T \mathbf{H}_{j+1}^T \cdots \mathbf{H}_K^T \right]^T \in \mathbb{C}^{\bar{N}_j \times N_b} \quad (16)$$

$$3: \quad \bar{\mathbf{H}}_j = \bar{\mathbf{U}}_j \bar{\Phi}_j \bar{\mathbf{W}}_j^H = \bar{\mathbf{U}}_j \bar{\Phi}_j \left[\bar{\mathbf{W}}_j^{(1)} \bar{\mathbf{W}}_j^{(0)} \right]^H \quad (16)$$

$$4: \quad \mathbf{P}_j^{c(CQA-BD)} = \bar{\mathbf{W}}_j^{(0)} \quad (15)$$

$$5: \quad \mathbf{P}_j^{c(RBD)} = \bar{\mathbf{W}}_j \left(\bar{\Phi}_j^T \bar{\Phi}_j + \chi \mathbf{I}_{N_b} \right)^{-1/2} \quad (20)$$

$$6: \quad \mathbf{H}_{e_j} = \mathbf{H}_j \mathbf{P}_j^c = \mathbf{U}_j \Phi_j \mathbf{W}_j^H = \mathbf{U}_j \begin{bmatrix} \Phi_j & 0 \\ 0 & 0 \end{bmatrix} \begin{bmatrix} \mathbf{W}_j^{(1)} & \mathbf{W}_j^{(0)} \end{bmatrix}^H \quad (22)$$

$$7: \quad \left(\Omega_j^{(CQA-BD, CQA-RBD)} \right)^{\frac{1}{2}} \text{ by classical WF [29] or variations}$$

$$8: \quad \mathbf{P}_j^{d(CQA-BD)} = \mathbf{W}_j^{(1)} \left(\Omega_j^{(BD)} \right)^{\frac{1}{2}} \quad (17)$$

$$9: \quad \mathbf{P}_j^{d(CQA-RBD)} = \mathbf{W}_j \left(\Omega_j^{(CQA-RBD)} \right)^{\frac{1}{2}} \quad (21)$$

$$10: \quad \mathbf{P}_j = \mathbf{P}_j^c \mathbf{P}_j^d \quad (12)$$

11: **end for**

$$12: \quad \mathbf{P} = [\mathbf{P}_1 \mathbf{P}_2 \cdots \mathbf{P}_K]^T \in \mathbb{C}^{N_b \times N_u} \quad (14)$$

uniform power allocation and then the CQA-MAAS power allocation is carried out.

IV. PROPOSED CQA-MAAS POWER ALLOCATION

In this section, we derive the proposed CQA-MAAS power loading algorithm to compute the matrix $\Gamma^{(CQA-BD)}$ based on the waterfilling principle [53]. Similar procedure can be pursued for obtaining $\Gamma^{(CQA-RBD)}$ and other linear precoders. In contrast to the design of the proposed CQA-BD and CQA-RBD precoders, the proposed CQA-MAAS power allocation does not lead to a unique solution and is only guaranteed to converge to a local optimum. Before starting the derivation, we consider the following essential properties and one theorem to facilitate its exposition:

- (i) Let \mathbf{A} be a matrix $\in \mathbb{C}^{m \times n}$, $m < n$, with rank $r \leq p = \min\{m, n\}$ [16].
 - a) It can be written as a product $\mathbf{S}\mathbf{Y}\mathbf{T}^H$, which is its SVD.
 - b) \mathbf{S} and \mathbf{T} have orthonormal columns, i.e., $\mathbf{S}^H \mathbf{S} = \mathbf{I}_m$ and $\mathbf{T}^H \mathbf{T} = \mathbf{I}_n$.
 - c) \mathbf{Y} has nonnegative elements on its main diagonal and zeros elsewhere.
- (ii) Assuming that k, k_1, k_2 are scalars and the sizes of the matrices $\mathbf{A}, \mathbf{B}, \mathbf{C}$ and \mathbf{E} are chosen so that each operation is well defined, we have [19]:
 - a) $k \mathbf{A} \mathbf{B} = (k \mathbf{A}) \mathbf{B} = \mathbf{A} (k \mathbf{B})$
 - b) $\mathbf{A} (\mathbf{B} + \mathbf{C}) = \mathbf{A} \mathbf{B} + \mathbf{A} \mathbf{C}$
 - c) $(\mathbf{B} + \mathbf{C}) \mathbf{A} = \mathbf{B} \mathbf{A} + \mathbf{C} \mathbf{A}$

$$\text{d) } k_1 (\mathbf{ABC}) + k_2 (\mathbf{AEC}) = \mathbf{A} [(k_1 \mathbf{B} + k_2 \mathbf{E}) \mathbf{C}]$$

(iii) Let \mathbf{F} and \mathbf{G} be $m \times n$ and $n \times m$ matrices, respectively. Then, the following identity holds:

$$\det(\mathbf{I}_m + \mathbf{FG}) = \det(\mathbf{I}_n + \mathbf{GF}) \text{ [18].}$$

(iv) Let $\mathbf{A} = [a_{ij}]$ be a non-negative $n \times n$ Hermitian matrix. Then, $\det(\mathbf{A}) \leq \prod_{i=1}^n a_{ii}$ with equality if and only if some $a_{ii} = 0$ or \mathbf{A} is diagonal [18].

$$\text{(v) } \log \det(\mathbf{A}) = \text{Tr} \log(\mathbf{A}), \forall \text{ nonsingular } \mathbf{A}^{n \times n} \text{ [20]}$$

$$\text{(vi) } \det(\mathbf{A}) = \prod_{i=1}^n \lambda_i \text{ where } \lambda_i \text{ denotes the } i\text{th eigenvalue of } \mathbf{A} \in \mathbb{C}^{n \times n} \text{ or } \mathbb{R}^{n \times n} \text{ [16].}$$

$$\text{(vii) } \log_2 \det(\mathbf{A}) = \sum_{i=1}^n \log_2(\mathbf{a}_{ii}), \quad \text{if } \mathbf{A} \text{ is diagonal}$$

and $\mathbf{a}_{ii} > 0$

We now resort to the expression of the achievable sum-rate of CQA precoding algorithms whose derivation is detailed in the Appendix:

$$C = \log_2 \left\{ \det \left[\mathbf{I}_{Nu} + \delta^2 (\mathbf{HP}) \mathbf{R}_s (\mathbf{HP})^H \right. \right. \\ \left. \left. \left((1 - \delta^2) (\mathbf{HP}) \mathbf{R}_s (\mathbf{HP})^H + N_0 \mathbf{I}_{Nu} \right)^{-1} \right] \right\} \quad (26)$$

where $\mathbf{R}_s = \mathbb{E}[\mathbf{ss}^H]$ denotes the covariance matrix associated to the symbol vector. The expression comprises a factor composed of the inverse of a sum of matrices, which is hard to deal with. An alternative approach to computing it would be a recursive procedure [15], which could not lead to a compact form. Since we aim to obtain closed-form expressions, we have opted for employing the following approximation based on Neumann's truncated matrix series [16], [17].

Theorem 2. *Let \mathbf{Q} represent an $n \times n$ matrix. Then, the infinite series $\mathbf{I} + \mathbf{Q} + \mathbf{Q}^2 + \mathbf{Q}^3 + \dots$ converges if and only if $\lim_{k \rightarrow \infty} \mathbf{Q}^k = \mathbf{0}$, in which case $\mathbf{I} - \mathbf{Q}$ is non-singular and*

$$(\mathbf{I} - \mathbf{Q})^{-1} = \sum_{k=0}^{\infty} (\mathbf{Q})^k \\ = \mathbf{I} + \mathbf{Q} + \mathbf{Q}^2 + \mathbf{Q}^3 + \dots \quad (27)$$

where $\mathbf{Q}^0 = \mathbf{I}$.

Replacing \mathbf{Q} by $(-\mathbf{Q})$, we have

$$(\mathbf{I} + \mathbf{Q})^{-1} = \sum_{k=0}^{\infty} (-\mathbf{Q})^k \\ = \mathbf{I} - \mathbf{Q} + \mathbf{Q}^2 - \mathbf{Q}^3 + \dots \quad (28)$$

Theorem 3. Let \mathbf{Q} represent an $n \times n$ matrix. If $\|\mathbf{Q}\| < 1$, where $\|\cdot\|$ denotes the Frobenius norm. Then, $\lim_{k \rightarrow \infty} \mathbf{Q}^k = \mathbf{0}$

Based on Theorem 3, we assume that (28) can provide accurate approximations if we truncate it after the second term. Then, we employ

$$(\mathbf{I} + \mathbf{Q})^{-1} \approx \mathbf{I} - \mathbf{Q}. \quad (29)$$

for rewriting (26) as follows:

$$\begin{aligned} C &= \log_2 \left\{ \det \left[\mathbf{I}_{Nu} + \frac{\delta^2}{N_0} (\mathbf{HP}) \mathbf{R}_s (\mathbf{HP})^H \right. \right. \\ &\quad \left. \left. \times \left(\mathbf{I}_{Nu} + \underbrace{\frac{\epsilon}{N_0} (\mathbf{HP}) \mathbf{R}_s (\mathbf{HP})^H}_{\mathbf{Q}} \right)^{-1} \right] \right\} \\ &\approx \log_2 \left\{ \det \left[\mathbf{I}_{Nu} + \frac{\delta^2}{N_0} (\mathbf{HP}) \mathbf{R}_s (\mathbf{HP})^H \right. \right. \\ &\quad \left. \left. - \frac{\delta^2 (1 - \delta^2)}{N_0} \left((\mathbf{HP}) \mathbf{R}_s (\mathbf{HP})^H \right)^2 \right] \right\} \end{aligned} \quad (30)$$

It can be noticed that the coefficient $\epsilon = \frac{(1 - \delta^2)}{N_0}$ constrains the norm of \mathbf{Q} matrix resulting from the Hermitian matrices product. For the analysis of the conditions and consequences of the previously assumed approximation, which is discussed in Subsection V-A, we define that coefficient as follows:

$$\epsilon = \frac{SNR (1 - \delta^2)}{Nu} \quad (31)$$

where we defined $N_0 = \frac{Nu}{SNR}$. It is well known [18] that the capacity for MIMO channels, subjected to ergodicity requirements, when \mathbf{H} is perfectly known at the receiver, can be expressed by

$$C = \log_2 \left\{ \det \left[\mathbf{I} + \frac{\mathbf{H} \mathbf{Q} \mathbf{H}^H}{\sigma_n^2} \right] \right\} \quad (32)$$

where $\sigma_n^2 = \mathbb{E} \{n(i) n^H(i)\}$ denotes the noise covariance. It is also shown in [18] that (32) is maximized when \mathbf{Q} is diagonalized, i.e., $\mathbf{Q} = \mathbf{W} \mathbf{\Omega} \mathbf{W}^H$, where $\mathbf{W} \in \mathbb{C}^{Nb \times Nb}$ denotes the unitary matrix containing the eigenvectors of $\mathbf{H} \mathbf{H}^H$ described by

$$\mathbf{\Omega} = \begin{bmatrix} \omega_{11} & 0 & \cdots & 0 \\ 0 & \omega_{22} & \cdots & 0 \\ \vdots & & \ddots & \\ 0 & \cdots & \cdots & \omega_{NN} \end{bmatrix} \quad (33)$$

where the total power is distributed among the diagonal entries of Ω , i.e., $\sum_{i=1}^N [\Omega]_{ii} = P_t$. For unquantized BD or RBD precoding algorithms, i.e., a full resolution one, we can expand (32) in terms of the N_j parallel sub channels obtained from the SVD of the non-interfering block channels (22) as follows:

$$C_{fr_j} = \log_2 \left\{ \det \left[\mathbf{I}_{N_j} + \frac{\mathbf{U}_j \Phi_j \mathbf{W}_j^H \mathbf{W}_j \Omega_j \mathbf{W}_j^H (\mathbf{U}_j \Phi_j \mathbf{W}_j^H)^H}{\sigma_n^2} \right] \right\} \quad (34)$$

We can use properties (i)b and (iii) to transform (34) into

$$C_{fr_j} = \log_2 \left\{ \det \left[\mathbf{I} + \frac{\Phi_j^2 \Omega_j}{\sigma_n^2} \right] \right\} \quad (35)$$

The total sum-rate for unquantized BD can be computed as the sum-rates of each user, as follows:

$$C_{fr} = \sum_{j=1}^K \log_2 \left\{ \det \left[\mathbf{I}_{N_j} + \frac{\Phi_j^2 \Omega_j}{\sigma_n^2} \right] \right\} \quad (36)$$

where we can neglect the $(N_b - N_u)$ right column vectors of $\Phi_j \in \mathbb{R}^{N_j \times [N_b - (N_u - N_j)]}$. Thus, we consider only the left main diagonal matrix, as indicated by

$$\Phi_j = \underbrace{\begin{bmatrix} \phi_{11} & 0 & \cdots & 0 \\ 0 & \phi_{22} & \cdots & 0 \\ \vdots & & \ddots & \vdots \\ 0 & \cdots & \cdots & \phi_{N_j N_j} \end{bmatrix}}_{\substack{N_j \text{ valid} \\ \text{diagonal matrix}}} \underbrace{\begin{bmatrix} 0 & \cdots & 0 \\ 0 & \cdots & 0 \\ \vdots & \cdots & \vdots \\ 0 & \cdots & 0 \end{bmatrix}}_{\substack{(N_b - N_u) \text{ null} \\ \text{vectors neglected}}} \quad (37)$$

In order to make the size of the power allocation matrix Ω_j described ahead compatible with the size of the singular values matrix Φ_j , we take into account only its upper left N_j diagonal matrix, which consists of the underbraced elements :

$$\Omega_j = \begin{bmatrix} \underbrace{\omega_{11}} & \bullet \bullet \bullet & 0 & 0 & \cdots & 0 \\ \vdots & \ddots & \vdots & \vdots & \ddots & \vdots \\ 0 & \bullet \bullet \bullet & \underbrace{\omega_{N_j N_j}} & 0 & \cdots & 0 \\ 0 & \cdots & 0 & 0 & \cdots & 0 \\ \vdots & \ddots & \vdots & \vdots & \ddots & \vdots \\ 0 & \cdots & 0 & 0 & \cdots & 0 \end{bmatrix} \quad (38)$$

The problem of power allocation for an unquantized BD algorithm can then be formulated as follows:

$$C_{fr} = \max_{\Phi_j} \sum_{j=1}^K \log_2 \left\{ \det \left[\mathbf{I}_{N_j} + \frac{\Phi_j^2 \Omega_j}{\sigma_n^2} \right] \right\}$$

$$\text{s.t. } \sum_{j=1}^K \text{Tr}(\Omega_j) \leq P_{total} \quad (39)$$

Now, we can expand the approximation in (30) by means of the N_j parallel sub channels obtained from the SVD of the non-interfering block channels (22). The procedure is similar to that used to obtain (34). For compactness, we use the notation $\det(\cdot) = |\cdot|$.

$$C_j \approx \log_2 \left| \mathbf{I}_{N_j} + \frac{\delta^2}{N_0} \mathbf{U}_j \Phi_j \mathbf{W}_j^H \mathbf{W}_j \Omega_j \mathbf{W}_j^H (\mathbf{U}_j \Phi_j \mathbf{W}_j^H)^H - \frac{\delta^2(1-\delta^2)}{N_0} (\mathbf{U}_j \Phi_j \mathbf{W}_j^H \mathbf{W}_j \Omega_j \mathbf{W}_j^H \times (\mathbf{U}_j \Phi_j \mathbf{W}_j^H))^2 \right| \quad (40)$$

By using properties (i)b and (ii)d, expression (40) can be simplified as follows:

$$C_j \approx \log_2 \left| \mathbf{I}_{N_j} + \mathbf{U}_j \left(\frac{\delta^2}{N_0} \Phi_j^2 \Omega_j - \frac{\delta^2(1-\delta^2)}{N_0^2} \Phi_j^4 \Omega_j^2 \right) \mathbf{U}_j^H \right|$$

$$= \log_2 \left| \mathbf{I}_{N_j} + \frac{\delta^2}{N_0} \Phi_j^2 \Omega_j - \frac{\delta^2(1-\delta^2)}{N_0^2} \Phi_j^4 \Omega_j^2 \right| \quad (41)$$

The argument of the determinant is composed of three terms, which are diagonal matrices composed of real entries and whose sum provides a real diagonal vector. This allows us to combine property (iv) with property (v) to formulate the maximization needed for power allocation of our proposed CQA-MAAS power allocation approach. The procedure is similar to that provided for obtaining the sum-rate for full resolution BD in (39), i.e.:

$$C \approx \max_{\Phi_j} \sum_{j=1}^K \log_2 \left| \mathbf{I}_{N_j} + \frac{\delta^2}{N_0} \Phi_j^2 \Omega_j - \frac{\delta^2(1-\delta^2)}{N_0^2} \Phi_j^4 \Omega_j^2 \right|$$

$$= \max_{\Phi_j} \sum_{j=1}^K \text{Tr} \left[\log_2 \left| \mathbf{I}_{N_j} + \frac{\delta^2}{N_0} \Phi_j^2 \Omega_j - \frac{\delta^2(1-\delta^2)}{N_0^2} \Phi_j^4 \Omega_j^2 \right| \right]$$

$$\begin{aligned}
& \left. - \frac{\delta^2 (1 - \delta^2)}{N_0^2} \Phi_j^4 \Omega_j^2 \right] \\
& \text{s.t. } \sum_{j=1}^K \text{Tr}(\Omega_j) \leq P_{total}
\end{aligned} \tag{42}$$

where Φ_j and Ω_j are expressed by (37) and (38), respectively.

Now, we can deal with the constrained optimization problem [29], [53], [55] in (42) with the method of Lagrange multipliers. To this end, we write the cost function as

$$\begin{aligned}
\Upsilon(\Omega_1, \dots, \Omega_K) = & \sum_{j=1}^K \text{Tr} \left[\log_2 \left| \mathbf{I}_{N_j} + \frac{\delta^2}{N_0} \Phi_j^2 \Omega_j \right. \right. \\
& \left. \left. - \frac{\delta^2 (1 - \delta^2)}{N_0^2} \Phi_j^4 \Omega_j^2 \right] + \beta \sum_{j=1}^K \text{Tr}(\Omega_j)
\end{aligned} \tag{43}$$

where β denotes the Lagrange multiplier. By using property (vii), we can convert (43) into

$$\begin{aligned}
\Upsilon(\Omega_1, \dots, \Omega_K) = & \sum_{j=1}^K \text{Tr} \begin{bmatrix} \log_2(d_{11}) & & \\ & \ddots & \\ & & \log_2(d_{nn}) \end{bmatrix}_j \\
& + \beta \sum_{j=1}^K \text{Tr} \begin{bmatrix} \omega_{11} & & \\ & \ddots & \\ & & \omega_{N_j N_j} \end{bmatrix}_j
\end{aligned} \tag{44}$$

where the subscript $(\cdot)_{nn}$ of the diagonal entries is associated with the n th receive antenna of the j th user. In the case of the first summand, we have

$$d_{nn} \Big|_{n=1, \dots, N_j} = 1 + \frac{\delta^2}{N_0} \phi_{nn}^2 \omega_{nn} - \frac{(\delta^2 - \delta^4)}{N_0^2} \phi_{nn}^4 \omega_{nn}^2 \tag{45}$$

We can combine (44) with (45) and maximize the resulting cost function associated with a generic n th receive antenna of the j th user as follows:

$$\frac{\partial \Upsilon(\omega_{nn})}{\partial \omega_{nn}} = \frac{1}{\ln(2)} \frac{1}{d_{nn}} \frac{\partial(d_{nn})}{\partial \omega_{nn}} + \beta \frac{\partial(\omega_{nn})}{\partial \omega_{nn}} = 0 \tag{46}$$

By solving (46), we can obtain the energy level, defined as

$$\mu = \frac{-1}{\beta \ln(2)} = \frac{N_0^2 + N_0 \delta^2 \phi_{nn}^2 \omega_{nn} - (\delta^2 - \delta^4) \phi_{nn}^4 \omega_{nn}^2}{N_0^2 \delta^2 \phi_{nn}^2 - 2(\delta^2 - \delta^4) \phi_{nn}^4 \omega_{nn}} \tag{47}$$

Note: From this point on, we will drop the subscripts $(\cdot)_{nn}$ for the sake of compactness.

After algebraic manipulations and rearranging terms in (47), we obtain the following second degree

equation:

$$\omega^2 - \frac{[N_0\delta^2\phi^2 + 2\mu(\delta^2 - \delta^4)\phi^4]}{(\delta^2 - \delta^4)\phi^4} \omega + \frac{\mu N_0\delta^2\phi^2 - N_0^2}{(\delta^2 - \delta^4)\phi^4} = 0, \quad (48)$$

where the distortion factor δ lies in the range $(0, 1)$. The solution of (48) can be arranged as follows:

$$\omega = \frac{N_0 + 2\mu(1 - \delta^2)\phi^2}{2(1 - \delta^2)\phi^2} \pm \frac{\sqrt{4\mu^2\delta^2(1 - \delta^2)^2\phi^4 + N_0^2(4 - 3\delta^2)}}{2\delta(1 - \delta^2)\phi^2}, \quad (49)$$

The procedure of squaring the second summand, which at a glance could be useful, would imply squared terms of individual powers ω^2 that would not satisfy the power constraint (42), which requires linear terms ω . Thus, we can express the radical as a McLaurin series truncated after the 4th term as follows:

$$\begin{aligned} f(\phi) &= \sqrt{4\mu^2\delta^2(1 - \delta^2)^2\phi^4 + N_0^2(4 - 3\delta^2)} \\ &\approx \sqrt{N_0(4 - 3\delta^2)} + \frac{2\mu^2\delta^2(1 - \delta^2)\phi^4}{N_0^2(4 - 3\delta^2)} \end{aligned} \quad (50)$$

where $f'(0) = f''(0) = f'''(0) = 0$. We can combine (50) with (49) to obtain the desired power expression:

$$\omega = \frac{N_0}{2(1 - \delta^2)\phi^2} + \mu \pm \left[\frac{N_0\sqrt{(4 - 3\delta^2)}}{2\delta(1 - \delta^2)\phi^2} + \frac{\mu^2\delta(1 - \delta^2)\phi^2}{N_0\sqrt{(4 - 3\delta^2)}} \right] \quad (51)$$

In order to ensure real levels of power, we choose the negative sign in (51) and rearrange it. In this way, we arrive at the can formulate the CQA-MAAS power allocation applied to each antenna of each user:

$$\omega_{nn}^{\text{MAAS}} \Big|_j = \left(C_1 N_0 \frac{1}{\phi^2} + \mu - \mu^2 C_2 \frac{1}{N_0} \phi^2 \right)^{(+)} \Big|_j \quad (52)$$

$$C_1 = \frac{\delta - \sqrt{4 - 3\delta^2}}{2\delta(1 - \delta^2)} \quad (53)$$

$$C_2 = \frac{\delta(1 - \delta^2)}{\sqrt{4 - 3\delta^2}} \quad (54)$$

where $(+)$ denotes the Kuhn-Tucker conditions:

$$(\omega_{nn})^+ = \omega, \quad \text{if } \omega_{nn} \geq 0 \quad (55)$$

$$0, \quad \text{if } \omega_{nn} < 0 \quad (56)$$

Now, we can write the constraint in (42) in matrix form as

$$\sum_{j=1}^K \text{Tr}(\Omega_j) = P_{\text{total}} = \sum_{j=1}^K \begin{bmatrix} \omega_{11} & & \\ & \ddots & \\ & & \omega_{N_j N_j} \end{bmatrix}_j$$

$$\begin{aligned}
&= \sum_{j=1}^K \text{Tr} \left\{ (C_1 N_0) \begin{bmatrix} \frac{1}{\phi_{11}^2} & & \\ & \ddots & \\ & & \frac{1}{\phi_{N_j N_j}^2} \end{bmatrix}_j \right\} \\
&+ \sum_{j=1}^K \text{Tr} \left\{ \mu \begin{bmatrix} 1 & & \\ & \ddots & \\ & & 1_{N_j N_j} \end{bmatrix}_j \right\} \\
&- \sum_{j=1}^K \text{Tr} \left\{ \mu^2 \left(\frac{C_2}{N_0} \right) \begin{bmatrix} \phi_{11}^2 & & \\ & \ddots & \\ & & \phi_{N_j N_j}^2 \end{bmatrix}_j \right\}
\end{aligned} \tag{57}$$

After rearranging terms, the matrix-form constraint (57) can be written as a second degree equation whose addends are in summation-form:

$$\begin{aligned}
&\mu^2 \left(\frac{C_2}{N_0} \right) \sum_{j=1}^K \sum_{l=1}^{N_j} [\phi^2]_{l,j} - \mu \sum_{j=1}^K \sum_{l=1}^{N_j} [1]_{l,j} \\
&+ P_t - (C_1 N_0) \sum_{j=1}^K \sum_{l=1}^{N_j} \left[\frac{1}{\phi^2} \right]_{l,j} = 0
\end{aligned} \tag{58}$$

The solutions of equation (58) can be expressed as:

$$\begin{aligned}
\mu &= \frac{N_u N_0}{2 C_2} \left(\frac{1}{\sum_{j=1}^K \sum_{l=1}^{N_j} [\phi^2]_{l,j}} \right) \\
&\pm \left[\left(\frac{N_u N_0}{2 C_2} \left(\frac{1}{\sum_{j=1}^K \sum_{l=1}^{N_j} [\phi^2]_{l,j}} \right) \right)^2 \right. \\
&\left. - \left(\frac{P_t N_0 - C_1 N_0^2 \sum_{j=1}^K \sum_{l=1}^{N_j} \left[\frac{1}{\phi^2} \right]_{l,j}}{C_2 \sum_{j=1}^K \sum_{l=1}^{N_j} [\phi^2]_{l,j}} \right) \right]^{\frac{1}{2}}
\end{aligned} \tag{59}$$

We can simplify the previous expression by considering (11) and recalling, from Section II, that $\mathbf{R}_{ss} \approx \mathbf{I}_{N_u}$. We can also assume that the total power is given by $P = \text{trace}(\mathbf{R}_{ss}) = N_u$, resulting in $N_0 = \frac{N_u}{\text{SNR}}$. The combination of this expression with (59) yields:

$$\begin{aligned}
\mu_{opt} &= \frac{N_u^2}{2 C_2 \text{SNR} \sum_{j=1}^K \sum_{l=1}^{N_j} [\phi^2]_{l,j}} \\
&\times \left\{ 1 - \left[1 + \frac{4 C_2}{N_u^2} \sum_{j=1}^K \sum_{l=1}^{N_j} [\phi^2]_{l,j} \right] \right\}
\end{aligned}$$

$$\times \left(-\text{SNR} + C_1 \sum_{j=1}^K \sum_{l=1}^{N_j} \left[\frac{1}{\phi^2} \right]_{l,j} \right) \right]^{\frac{1}{2}} \} \quad (60)$$

where we choose the negative sign before the square root in (59) to ensure the appropriate smallest positive levels of power. In summary, the following steps can describe the iterative process of the CQA-MAAS for power allocation, which is a customization of the classical Waterfilling method [53], [29], [55] for low-resolution signals. The procedure is derived from expressions (60) and (52). We start with the first one (60), which can be converted into:

$$\begin{aligned} \mu_{opt} &= \frac{(N_u - p + 1)^2}{2C_2\text{SNR} \sum_{m=1}^{(N_u-p+1)} [\phi^2]_m} \\ &\times \left\{ 1 - \left[1 + \frac{4C_2}{N_u^2} \sum_{m=1}^{(N_u-p+1)} [\phi^2]_m \right. \right. \\ &\times \left. \left. \left(-\text{SNR} + C_1 \sum_{m=1}^{(N_u-p+1)} \left[\frac{1}{\phi^2} \right]_m \right) \right]^{\frac{1}{2}} \right\}, \end{aligned} \quad (61)$$

where

- (i) N_u stands for the number of receive antennas defined in Section II.
- (ii) p denotes an auxiliary parameter to be set to 1.
- (iii) C_1 and C_2 , which depend only on the distortion factor δ , are given by (53) and (54).
- (iv) ϕ designates each of the $N_u = K \times N_j$ singular values corresponding to each receive antenna. This can be better visualized in the following diagonal matrix (33), in which the diagonal vector displays the required entries $\phi_m \in \phi_1, \dots, \phi_{N_u}$.

$$\Phi = \begin{bmatrix} \phi_1 & \cdots & 0 & \cdots & 0 & \cdots & 0 \\ \vdots & \ddots & \vdots & & \vdots & \ddots & \vdots \\ 0 & \cdots & \phi_{N_j} & \cdots & 0 & \cdots & 0 \\ \vdots & & \vdots & \ddots & \vdots & & \vdots \\ \vdots & & \vdots & & \vdots & & \vdots \\ 0 & \cdots & 0 & \cdots & \phi_{(N_u-N_j)} & \cdots & 0 \\ \vdots & \ddots & \vdots & & \vdots & \ddots & \vdots \\ 0 & \cdots & 0 & \cdots & 0 & \cdots & \phi_{N_u} \end{bmatrix} \quad (62)$$

Employing the value of μ_{opt} provided by (61), the power allocated to the m th $\in \{1, \dots, N_u\}$ receive antenna can be computed by

$$\begin{aligned} \omega_m &= C_1 \frac{(N_u - p + 1)}{\text{SNR}} \frac{1}{\phi_m^2} + \mu_{opt} \\ &- \mu_{opt}^2 C_2 \frac{\text{SNR}}{(N_u - p + 1)} \phi_m^2 \end{aligned} \quad (63)$$

where the parameters involved were defined in (i), (ii), (iii) and (iv). Assuming that the power allotted to the receive antenna which is associated to the minimum gain is negative, i.e., $\omega_{N_u-p+1} < 0$, it is rejected, and the algorithm must be executed with the parameter p increased by unity. The most advantageous allotment strategy is achieved at the time that the power distributed among each receive antenna is non-negative.

Here, we sum up the CQA-MAAS power allocation algorithm, which aims to compute $\Omega_j^{(BD)}$ (17), in Algorithm (2). For this purpose we can form a larger power diagonal matrix, where each of its N_u entries is associated to its corresponding j th user, in ascending order, as follows:

$$\Omega^{(BD)} = \text{diag}\{\Omega_1, \dots, \Omega_K\}, \quad (64)$$

which means that

$$\Omega^{(BD)} = \begin{bmatrix} \omega_1 & \cdots & 0 & \cdots & 0 & \cdots & 0 \\ \vdots & \ddots & \vdots & & \vdots & \ddots & \vdots \\ 0 & \underbrace{\cdots}_{\Omega_1} & \omega_{N_j} & \cdots & 0 & \cdots & 0 \\ \vdots & & \vdots & \ddots & \vdots & & \vdots \\ \vdots & & \vdots & & \vdots & & \vdots \\ 0 & \cdots & 0 & \cdots & \omega_{(N_u-N_j)} & \cdots & 0 \\ \vdots & \ddots & \vdots & & \vdots & \ddots & \vdots \\ 0 & \cdots & 0 & \cdots & 0 & \underbrace{\cdots}_{\Omega_K} & \omega_{N_u=K \times N_j} \end{bmatrix} \quad (65)$$

Moreover, according to [23] [24], we can combine (65) with (17), (12), (15) and (14), to incorporate

Algorithm 2 Proposed CQA-MAAS power allocation

- 1: **Initialization** : N_u, N_b, K
 2:

$$\Phi = \begin{bmatrix} \phi_1 & \cdots & 0 \\ \vdots & \ddots & \vdots \\ 0 & \cdots & \phi_{N_u} \end{bmatrix} \quad (62)$$

- 3: **Compute** the factors C_1 in (53) and C_2 in (54).
 4: **Compute** the optimum energy level μ_{opt} in (60).
 5: **Compute** the power allocation to each sub-channel ω_m in (63).
 6: **If** there are negative values, then find their minimum, i.e., their $\min(\omega_{N_u-p+1} < 0)$ **and**.
 7: **Refuse** this minimum negative value by assuming it is equal to zero in (56), **and**.
 8: **Perform** the algorithm with the parameter p incremented by unity.
 9: CQA-MAAS achieves its goal when the power allocated among the receive antennas is non-negative (56).
 10: **Compute** the power diagonal matrix (65), by relating its N_u power entries to their corresponding receive antennas.
-

CQA-MAAS into the precoding matrix, expressed in terms of each user as follows:

$$\begin{aligned} \mathbf{P}_{opt}^{BD} &= \left[\overline{\mathbf{W}}_1^{(0)} \mathbf{W}_1^{(1)} \left(\Omega_1^{(BD)} \right)^{\frac{1}{2}} \cdots \overline{\mathbf{W}}_K^{(0)} \mathbf{W}_K^{(1)} \left(\Omega_K^{(BD)} \right)^{\frac{1}{2}} \right] \\ &= \left[\overline{\mathbf{W}}_1^{(0)} \mathbf{W}_1^{(1)} \cdots \overline{\mathbf{W}}_K^{(0)} \mathbf{W}_K^{(1)} \right] \left(\Omega^{(BD)} \right)^{\frac{1}{2}} \end{aligned} \quad (66)$$

V. ANALYSIS

In this section, we analyze aspects of the approximation via Neumann's series, which is employed in the formulation of the proposed CQA-MAAS power allocation. We also examine the achievable sum-rate of the proposed CQA precoding and power allocation techniques along with their computational complexity. Moreover, we assess the power consumption of the proposed and existing approaches.

A. Maximum accurate SNR under CQA-MAAS

In this section, we estimate the maximum SNR for which the approximation proposed in (29) provides accurate values of the sum rate in (30). In (30) and (31) of Section IV, we stated that the parameter ϵ confines the norm of the Hermitian matrices product, which is denoted by \mathbf{Q} . It can be seen in [16] that the norm of a product between a constant c and a matrix $\mathbf{Q} \in \mathcal{C}^{m \times n}$ obeys $\|c \mathbf{Q}\| = |c| \|\mathbf{Q}\|$, where $|\cdot|$ stands for the modulus. Moreover, ϵ (31) plays the role of c previously described, which can be viewed as a norm shortener. Thus, we are interested in its small values that satisfy the limitation imposed by the theorem in 3 to validate the approximation in (30). In light of the assumed broadcast system, we focus on two configurations, $N_b = 64$ and $N_u = 8 \times 2$ and $N_b = 64$ and $N_u = 16 \times 2$, which are examined in the simulations in Section VI. We also assume an arbitrary value $\epsilon \leq 0.01$.

The maximum SNR for which the approximation proposed in (30) provides accurate values of sum rates can be obtained by

$$\frac{\text{SNR}(1 - \delta^2)}{N_u} \leq 0.01 \quad (67)$$

which after manipulations, yields

$$\text{SNR (dB)}_{max} = 10 \log_{10} \frac{0.01 N_u}{(1 - \delta^2)} \quad (68)$$

Then, based on (68) and the two MU-MIMO configurations mentioned before, we can build the following table: Table I can be used to roughly estimate the region of the SNR range from which CQA-BD-MAAS

TABLE I
MAXIMUM ACCURATE SNR FOR TWO MU-MIMO CONFIGURATIONS: 1) $N_b = 64$ AND $N_u = 8 \times 2$; 2) $N_b = 64$ AND $N_u = 16 \times 2$

Quantization bits	δ	$N_b = 64$ $N_u = 8 \times 2$	$N_b = 64$ $N_u = 16 \times 2$
2	0.9387	1.2915	4.3018
3	0.9811	6.3075	9.3178
4	0.9942	11.4092	14.4195
5	0.9983	16.7301	19.7404
6	0.9995	22.0243	25.0525

starts to lose efficiency in terms of achievable sum rates, as will be shown in Fig.4 and Fig.5, in Section VI.

B. Achievable sum-rates

It is feasible to compute approximations of achievable sum-rates for downlink channels in which N_b and N_u are sufficiently large as both the error resulting from the combination of multiuser interference (MUI) and the quantization error from limited resolution of DACs can be considered as Gaussian [8]. This assumption, which is justified by the central limit theorem enables us to convert (9) into the matrix:

$$\mathbf{T}_{n,n} = \delta \mathbf{I}_{N_b \times N_b} \quad (69)$$

where the entries of $\mathbf{T}_{n,n}$ are given by the Bussgang scalar factor:

$$\delta = \alpha \gamma \sqrt{\frac{N_b}{\pi P}} \sum_{l=1}^{J-1} \exp\left(-\frac{N_b \gamma^2}{P} \left(1 - \frac{J}{2}\right)^2\right) \quad (70)$$

where the factor α is obtained by

$$\alpha = \left(2N_b \gamma^2 \left(\left(\frac{J-1}{2}\right)^2 - 2 \sum_{l=1}^{J-1} \left(1 - \frac{J}{2}\right) \Xi\left(\sqrt{2N_b \gamma^2} \left(1 - \frac{J}{2}\right)\right)\right)\right)^{-1/2} \quad (71)$$

where $\Xi(w) = \int_{-\infty}^w \frac{1}{\sqrt{2\pi}} \exp^{-v^2/2} dv$ [8] is the distributed function of a Gaussian random variable. We have followed the approach of [8] that considers the same sampling rates at both transmitter and receiver and that the DACs have coarse quantization but the ADCs have infinite quantization in order to focus on the effects of the DACs. In [14][Appendix], assuming the system model in Section II and the identity in (69), we have derived the following closed-form approximation for the sum rate achieved by CQA-BD and CQA-RBD precoders via Bussgang's theorem:

$$C = \log_2 \left\{ \det \left[\mathbf{I}_{N_u} + \delta^2 \frac{SNR}{N_u} (\mathbf{HP})(\mathbf{HP})^H \left((1 - \delta^2) \frac{SNR}{N_u} (\mathbf{HP})(\mathbf{HP})^H + \mathbf{I}_{N_u} \right)^{-1} \right] \right\} \quad (72)$$

where the SNR was defined in (10) and \mathbf{P} is the precoding matrix (14), which is defined in Section III.

Note that the quantization effect is concentrated on the Bussgang's factor δ in (69) and (70), which approximates the effects of quantization with few bits.

C. Power consumption and efficient DACs

Until recently, the use of a modest number of antennas at the BS and their required DACs were not an issue in terms of energy consumption. This is due to the fact that DACs consume less energy than ADCs. Despite the diversity of research about DACs, very few allow the calculation of the increment of chip power dissipation as bit resolution increases bit-by-bit for a given technology. In order to roughly compare the consumption of both equipments, we make use of Table II, which contains, in black, the fabrication parameters for GaAs 4-bit Analog-to-Digital Converter (AD) and 5-bit Digital-to-Analog (DA) converters, using a 0.7- μm MESFET self-aligned gate process [51] and the expression proposed in [52].

TABLE II
ADC AND DAC FABRICATION PARAMETERS WITH THE SAME TECHNOLOGY -INFERRED APPROXIMATED DATA IN RED

	Resolution (bits)	Sampling Rate (GHz)	Power dissipation (mW)
DAC	4	1	≈ 42.5
ADC	4	1	140
DAC	5	1	85
ADC	5	1	≈ 280
DAC	6	1	≈ 170
ADC	6	1	≈ 560
DAC	12	1	≈ 10880
ADC	12	1	≈ 35840

We start with the expression[52] which relates the power consumed by an ADC to the resolution in bits as follows:

$$P_{\text{ADC}}(b) = c \tau 2^b \quad (73)$$

where b stands for the resolution in bits, c is a constant and τ is the sampling rate. From (73), we obtain $\frac{P_{\text{ADC}}(4)}{P_{\text{ADC}}(5)} = \frac{1}{2}$, which allows us to estimate $\frac{P_{\text{DAC}}(5)}{P_{\text{ADC}}(5)} = \frac{P_{\text{DAC}}(5)}{2P_{\text{ADC}}(4)}$. With the help of Table II, we obtain $P_{\text{DAC}}(5) \approx 30\%P_{\text{ADC}}(5)$. So, the DAC consumes around 30 % of the energy of the ADC with fixed parameter. From the results obtained before, we can roughly estimate the economy in energy by assuming that similarly to ADC, DAC consumption doubles with every extra bit of resolution, i.e., of $\mathcal{O}(2^b)$. Therefore, a decrease in 6 resolution bits, for instance from 12 to 6 bits, represents a 98.4% lower consumption. This reduction of DAC consumption motivates our study. Following the above reasoning, we can add the estimated DAC data with \approx to Table II.

D. Computational complexity

This subsection is devoted to the comparison of the computational complexity of the proposed and existing precoders in terms of required floating point operations (FLOPs). For this purpose, we will make use of

the big O notation, i.e., $\mathcal{O}(\cdot)$. The number of FLOPs required by conventional BD and RBD algorithms are dominated by two SVDs [23]. Since our system model is dedicated to broadcast channels, we can assume the widespread ratios $N_b \gg N_u \gg N_j$ and one of their resulting approximations $N_u - N_j \approx N_u$ to simplify the resulting expressions. Table III illustrates the computational cost required by the proposed CQA and existing precoders.

TABLE III
COMPUTATIONAL COMPLEXITY OF PROPOSED CQA AND EXISTING PRECODING ALGORITHMS

Precoder	Computational cost (FLOPs) under $N_b \gg N_u \gg N_j$
ZF	$\frac{N_b^3}{2} + N_b^2 (4N_u - \frac{3}{2}) - N_b (N_u)$
MMSE	$\frac{N_b^3}{2} + N_b^2 (4N_u - \frac{3}{2}) - N_b (N_u - 2)$
BD	$N_b^2 (32N_j + 8) + N_b (32N_u^2 + 72N_j^2) + 64N_u^2$
RBD	$N_b^2 (32N_j + 8) + N_b (32N_u^2 + 72N_j^2) + 64N_u^2$
Bussgang ZF	$\frac{N_b^3}{2} + N_b^2 (4N_u - \frac{3}{2}) - N_b (N_u) + C_\delta$
Bussgang MMSE	$\frac{N_b^3}{2} + N_b^2 (4N_u - \frac{3}{2}) - N_b (N_u - 2) + C_\delta$
Proposed CQA-BD	$N_b^2 (32N_j + 8) + N_b (32N_u^2 + 72N_j^2) + 64N_u^2 + C_\delta$
Proposed CQA-RBD	$N_b^2 (32N_j + 8) + N_b (32N_u^2 + 72N_j^2) + 64N_u^2 + C_\delta$

The extra cost C_δ required to convert ZF, MMSE, BD and RBD into their corresponding Bussgang-based precoders, which are listed in Table III, do not have significant impact on the total computational cost of their respective Bussgang-based algorithms. Due to their design, existing waterfilling and the proposed CQA-MAAS power allocation have a similar computational cost of $\mathcal{O}(N_u)$, which in practice does not result in significant additional cost to be imposed on BD and RBD to obtain their respective CQA-BD-MAAS and CQA-RBD-MAAS schemes. Table IV depicts the complexity of the proposed CQA-MAAS technique and existing WF power allocation. A key advantage of BD-type precoders like the proposed CQA-BD and CQA-RBD algorithms over ZF and MMSE techniques is that due to their required SVDs they originate a power loading matrix that can be readily adjusted by power allocation algorithms. Therefore, the SVDs cost can be associated with the the precoders, whereas the power allocation algorithms adjust the power loading matrix resulting from the SVDs and require a reduced computational cost, $\mathcal{O}(N_u)$.

TABLE IV
COMPUTATIONAL COMPLEXITY OF PROPOSED CQA-MAAS AND EXISTING WF ALGORITHMS.

Technique	Computational cost (FLOPs)
Waterfilling (WF)	$\mathcal{O}(N_u)$
MAAS	$\mathcal{O}(N_u)$

VI. NUMERICAL RESULTS

In this section, we evaluate the performance of the proposed CQA precoding techniques and the CQA-MAAS power allocation strategy against the existing ZF, MMSE, BD and RBD precoders with full resolution and

the Bussgang ZF and MMSE precoders [8], [9] with coarsely-quantized signals using simulations. We remark that we have only considered narrowband systems with flat fading channels, whereas the work in [9] considered frequency-selective channels with a multicarrier MIMO setting that employs Bussgang ZF and MMSE precoders per subcarrier. These precoders when applied per subcarrier in a multicarrier MIMO system are equivalent to the same precoders used for narrowband MIMO systems with flat fading channels. We also consider the influence of imperfect channel knowledge and spatial correlation on the sum-rates of our proposed algorithms. Although the acronyms employed in the figures have already been defined, for clarity, we list them here along with short explanations:

- 1) CQA-MAAS: proposed power allocation strategy with coarsely quantized signals.
- 2) BD-FR: unquantized block-diagonalization algorithm that employs full resolution.
- 3) ZF-FR: unquantized zero-forcing algorithm that employs full resolution.
- 4) BD-FR_{plus} WF: unquantized block-diagonalization algorithm that employs full resolution plus existing WF [53], [18], [29].
- 5) CQA-BD: proposed block-diagonalization algorithm with coarsely quantized signals without MAAS.
- 6) CQA-BD-MAAS: proposed block-diagonalization algorithm with coarsely quantized signals with MAAS.
- 7) PCH and ICH: perfect and imperfect channel knowledge, respectively.

We focus on two scenarios, whose MU-MIMO configurations are $(N_b = 64, N_u = 8 \times 2)$ and $(N_b = 64, N_u = 16 \times 2)$ respectively. We model the channel matrix \mathbf{H}_j of the j th user with entries given by complex Gaussian random variables with zero mean and unit variance. Additionally, it is assumed for simplicity that the channel is static during the transmission of each packet and that the antennas are uncorrelated. The channel is first considered perfectly known to the transmitter in the case of CQA-BD and to both receiver and transmitter when using CQA-MAAS. We set the number of independent trials to 5×10^2 and the number of channels to 10^2 symbols. Fig.2 depicts the sum-rates of the proposed CQA-BD algorithm, and its variant equipped with CQA-MAAS, i.e., CQA-BD-5bits and CQA-BD-MAAS-5bits, respectively, according to the first scenario, i.e., $(N_b = 64, N_u = 8 \times 2)$. We recall that CQA-BD-MAAS-5bits is based on an approximation (29) obtained from a Neumann's truncated series. For comparison, we have also included the sum-rates of the BD-FR-_{plus existing} WF, which in this specific study, can be considered an upperbound for BD-type algorithms, and the existing BD-FR and ZF-FR precoding techniques, both under full resolution. It can be noticed that the following performance hierarchy is preserved over the considered range: BD-FR-_{plus existing} WF \geq CQA-BD-MAAS-5bits \geq BD-FR \geq ZF-FR \geq CQA-BD-5bits \geq Bussgang ZF-5bits. We can also observe the significant gap between CQA-BD-5bits and CQA-BD-MAAS-5bits, resulting from the incorporation of CQA-MAAS into CQA-BD-5bits. This gain in terms of achievable sum-rate, which is obtained for low SNR,

remains highly satisfactory over the remaining range of values. We also notice that the proposed CQA-BD algorithm outperforms the Bussgang-ZF algorithm [14] by up to 3dB for the same performance. Additionally, CQA-BD-MASS-5bits and BD-FR-plus existing WF are very close in the range $[-10 \ 7)$ dB, whereas in the range $[7 \ 15]$ dB the gap between them is very small. This gap decreases in a scenario composed of more receive antennas and also in the event of more quantization bits.

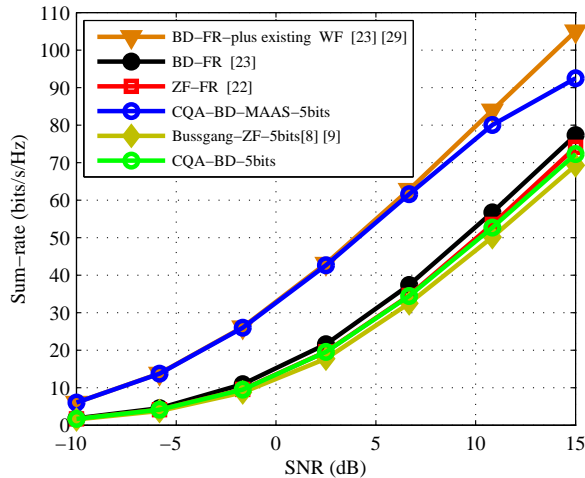


Fig. 2. Achievable rates for CQA-BD and CQA-BD-MAAS, 5quantization bits, via Bussgang theorem, Gaussian signals, compared to ZF-FR, BD-FR and BD-FR-plus existing WF. MU-MIMO configuration: $N_b = 64$ and $N_u = 8 \times 2$.

Fig.3 illustrates the sum-rate performance in the second configuration mentioned before, i.e. ($N_b = 64, N_u = 16 \times 2$). In this setting, in which we maintain the levels of quantization, in the range $[-1.6 \ 15]$ dB all curves displayed move up, reaching higher sum-rates. Their ranking, which is defined by the inequalities commented on previous figure remains the same, however, considering from the bottom to the top, the first group of curves composed of Bussgang ZF-5bits, CQA-BD-5bits, ZF-FR and BD-FR are closer to the first one, comprised by CQA-BD-MASS-5bits and BD-FR-MAAS. It can also be noticed that the two last mentioned curves, which in the prior figure, were already very close in the range $[-10 \ 6.6)$ dB, now become closer from 6.6dB to 15dB.

In Fig.4, which corresponds to the first scenario, i.e., ($N_b = 64, N_u = 8 \times 2$), it is shown the effect of the increase in the number of quantization bits on the performance of the proposed CQA-BD-MASS in the considered range of SNR. In order to better assess its effectiveness, we have also plotted BD-FR. CQA-BD-MASS-6bits clearly works as well as its upperbound BD-FR-plus existing WF.

In Fig.5, we assess the degree in which the sum-rates increase when the level of quantization varies in the second configuration, i.e., ($N_b = 64, N_u = 16 \times 2$). Both CQA-BD-MASS-6bits and CQA-BD-MASS-5bits are closer to BD-FR-MAAS. The performance of CQA-BD-MASS achieved in this scenario under 5 and 6bits quantization cannot be only justified by the increase in the levels of quantization, but also by the extra receive antennas. It can be noticed that the size of the coefficient ϵ defined in (31) is a condition of the

approximation (30) provided by Theorem 3. In other words, a decrease in ϵ resulting from an increased number of receive antennas leads to more accurate approximations of the sum-rate computed by (30).

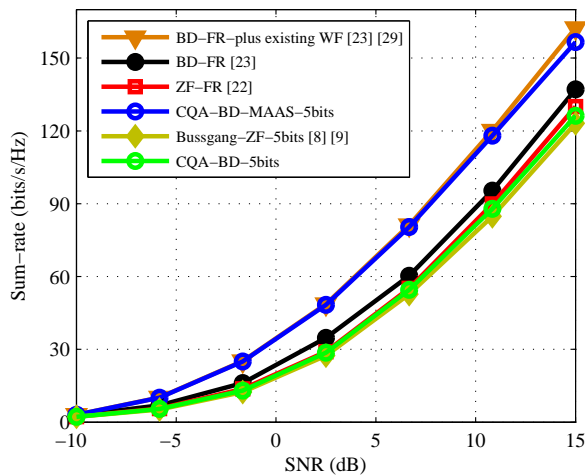


Fig. 3. Achievable rates for CQA-BD and CQA-BD-MAAS, 5 quantization bits, via Bussgang theorem, Gaussian signals, compared to ZF-FR, BD-FR and BD-FR-plus existing WF. MU-MIMO configuration: $N_b = 64$ and $N_u = 16 \times 2$.

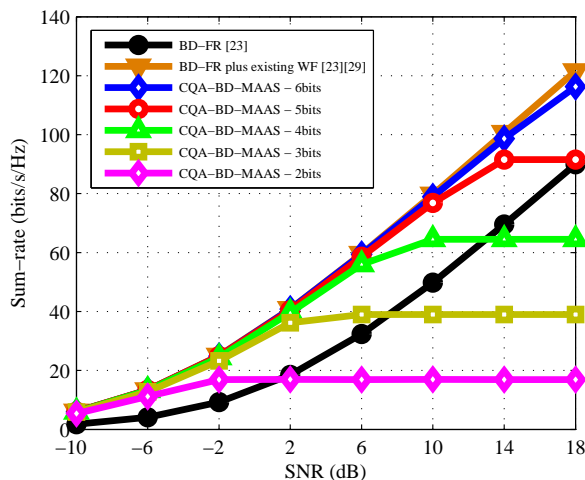


Fig. 4. Achievable rates for CQA-BD-MAAS, 2, 3, 4, 5, 6 quantization bits, via Bussgang theorem, Gaussian signals, compared to BD-FR and BD-FR-plus existing WF. MU-MIMO configuration: $N_b = 64$ and $N_u = 8 \times 2$.

Fig.6 illustrates the closeness between CQA-RBD-MAAS-5bits and its theoretical upper bound, RBD-FR-plus existing WF and the gain that CQA-MAAS incorporates into CQA-RBD-5bits to convert it into CQA-RBD-MAAS-5bits. We have also included RBD-FR, CQA-BD-5bits and Bussgang MMSE-5bits for comparisons. We can observe that, except for the neighborhood of -5 dB, the following non strict inequalities are preserved over the considered range in a similar way to that in Fig.2: $\text{RBD-FR-plus existing WF} \geq \text{CQA-RBD-MAAS-5bits} \geq \text{RBD-FR} \geq \text{CQA-RBD-5bits} \geq \text{Bussgang MMSE-5bits} \geq \text{CQA-BD-5bits}$. The large gap between CQA-RBD-MAAS-5bits and CQA-RBD-5bits in the range $[-1.6 \quad 15]$ dB and also its closeness to its theoretical upperbound, i.e., RBD-FR plus existing WF, make clear the effectiveness of the proposed CQA-MAAS power allocation combined with the Bussgang

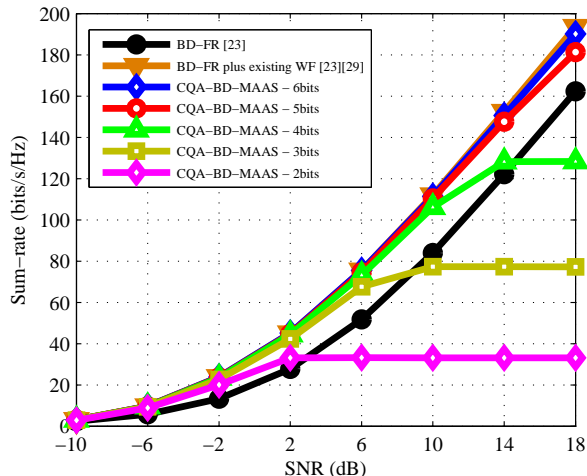


Fig. 5. Achievable rates for CQA-BD-MAAS, 2, 3, 4, 5, 6 quantization bits, via Busgang theorem, Gaussian signals, compared to that reached by BD-FR and BD-FR-plus existing WF. MU-MIMO configuration: $N_b = 64$ and $N_u = 16 \times 2$.

theorem for quantized signals applied to RBD algorithms.

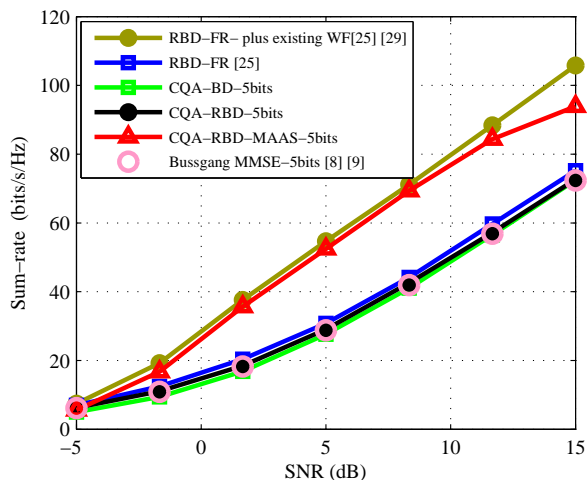


Fig. 6. Achievable rate for CQA-RBD-MAAS-5bits, via Busgang theorem, Gaussian signals, compared to that reached by CQA-RBD-5bits, CQA-BD-5bits, RBD-FR and RBD-FR-plus existing WF. MU-MIMO configuration: $N_b = 64$ and $N_u = 8 \times 2$.

In the example shown in Fig.7, we compare the proposed CQA-BD-MAAS-5bits to variations of 5bit-quantized BD algorithms, which employ traditional quantization, i.e., they are not based on Busgang theorem. It is also plotted BD-FR-plus existing WF as their theoretical upperbound. We have discarded a possible curve representing BD for $Q(\mathbf{P} \times \mathbf{s})$ -5bits plus existing WF due to its poor performance. The closeness of the proposed CQA-RBD-MAAS-5bits to its upperbound BD-FR-plus existing WF and the huge gap between it and the BD for $Q(\mathbf{H})$ -5bits plus existing WF in all considered range make clear its impressive performance.

We now consider the impact of practical aspects. Specifically, we have considered the model for imperfect channel knowledge and spatial correlation $\hat{\mathbf{H}} = \mathbf{H} \tilde{\mathbf{R}}^{\frac{1}{2}} + \mathbf{E}$, where $\tilde{\mathbf{R}}$ represents the complex transmit

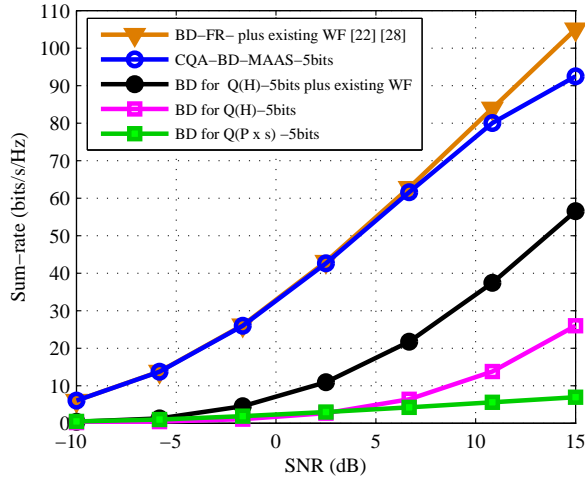


Fig. 7. Achievable rate for CQA-BD-MAAS-5bits, via Bussgang theorem, Gaussian signals, compared to that provided by BD-FR-plus existing WF, BD for 5bit-quantized precoded signal and BD for 5bit-quantized channel plus existing WF. MU-MIMO configuration: $N_b = 64$ and $N_u = 8 \times 2$.

correlation matrix [58], [27] whose elements are

$$\tilde{R}_{ij} = \begin{cases} r^{j-i}, & i \leq j \\ r_{ji}^*, & i > j \end{cases}, |r| \leq 1 \quad (74)$$

where $|r| < 1$. It can be noticed that the absolute values of the entries $|\tilde{R}_{(i,j)}|$ corresponding to the closest antennas are larger than the others. The error matrix \mathbf{E} is modeled [27] as a complex Gaussian noise with i.i.d entries of zero mean and variance σ_e^2 . In our next examples, we have employed large values of correlations between the neighboring antennas, i.e., $|r| = 0.72$ and 0.91 , respectively. The variance σ_e^2 of the feedback error matrix \mathbf{E} has been set to 0.16.

In Fig. 8, we assess the performance of CQA-BD and CQA-BD-MAAS in the presence of imperfect channel knowledge and spatial correlation using 3 and 6 bits. The results show that the impact of imperfect channel knowledge is not significant in terms of performance degradation of the precoders. However, the performance degradation of CQA-BD-MAAS can become significant for 3 bits.

In Fig. 9, we assess the performance of CQA-BD and CQA-RBD in the presence of imperfect channel knowledge and spatial correlation using 2 and 3 bits. The results show that CQA-RBD outperforms CQA-BD and the advantage of CQA-RBD in performance is more pronounced for scenarios with imperfect channel knowledge, which indicates the increased robustness of CQA-RBD. Specifically, the sum-rate performance of CQA-RBD is up to 30% higher than that of CQA-BD in scenarios with imperfect channel knowledge.

VII. CONCLUSIONS

We have proposed the CQA-BD and CQA-RBD precoding and the CQA-RBD-MAAS power allocation al-

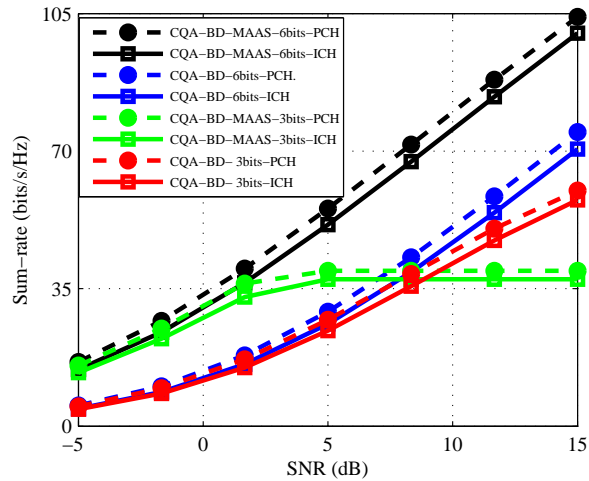


Fig. 8. Achievable rates for CQA-BD and CQA-BD-MAAS for 6 and 3-bit quantization under perfect and imperfect channel knowledge. MU-MIMO configuration: $N_b = 64$ and $N_u = 8 \times 2$. $|r| = 0.72$ and $\sigma_e^2 = 0.16$.

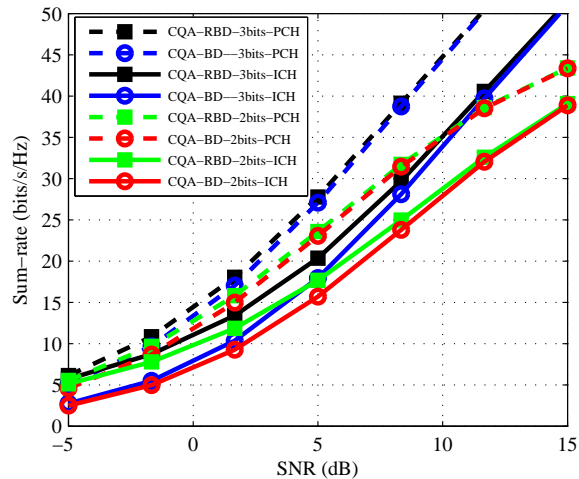


Fig. 9. Achievable rates for CQA-RBD and CQA-BD for 2 and 3-bit quantization, under perfect and imperfect channel knowledge. MU-MIMO configuration: $N_b = 64$ and $N_u = 8 \times 2$. $|r| = 0.91$ and $\sigma_e^2 = 0.16$.

gorithms for massive MIMO systems that employ coarse quantization using DACs with few bits. The proposed CQA-BD and CQA-RBD precoding algorithms outperform existing Bussgang-ZF and Bussgang-MMSE precoders for systems with coarse quantization, resulting in sum-rate gains of up to 15% while requiring a comparable computational cost. Moreover, CQA-RBD-MAAS can obtain gains in sum-rate of up to 30 % over schemes without power allocation and comparable performance to full-resolution schemes with precoding and WF power allocation. These findings include scenarios with perfect and imperfect channel knowledge as well as spatial correction between antennas. Finally, the proposed algorithms can be used in massive MIMO systems and contribute to substantial reduction in power consumption.

APPENDIX

Here we provide the derivation of (72).

A. Assumptions

According to Subsection II, we assume that the cross covariance matrices $\mathbf{R}_{sf} = \mathbb{E}[\mathbf{s}\mathbf{f}^H]$ and $\mathbf{R}_{sn} = \mathbb{E}[\mathbf{s}\mathbf{n}^H]$ and $\mathbf{R}_{fn} = \mathbb{E}[\mathbf{f}\mathbf{n}^H]$ are all equal to zero and so are \mathbf{R}_{fs} , \mathbf{R}_{ns} and \mathbf{R}_{nf} . Additionally, the distortion vector is assumed to be Gaussian.

B. Development

We start by combining (1) with (8), obtaining:

$$\mathbf{y} = \mathbf{H}\mathbf{T}\mathbf{P}\mathbf{s} + \mathbf{H}\mathbf{f} + \mathbf{n}, \quad (75)$$

where we can define a distortion-plus-noise vector

$$\tilde{\mathbf{n}} = \mathbf{H}\mathbf{f} + \mathbf{n}. \quad (76)$$

We can estimate the correlation matrix \mathbf{R}_{sqsq} of the quantized vector (8), as follows:

$$\begin{aligned} \mathbf{R}_{sqsq} &= \mathbb{E}[(\mathbf{T}\mathbf{P}\mathbf{s} + \mathbf{f})(\mathbf{T}\mathbf{P}\mathbf{s} + \mathbf{f})^H] \\ &= \mathbb{E}[\mathbf{T}\mathbf{P}\mathbf{s}\mathbf{s}^H\mathbf{P}^H\mathbf{T}^H + \mathbf{f}\mathbf{f}^H] \\ &= \delta^2\sigma_s^2\mathbf{P}\mathbf{P}^H + \mathbf{R}_{ff}, \end{aligned} \quad (77)$$

where we made use of (69) and the autocorrelation matrix of the symbol vector $\mathbf{R}_{ss} = \mathbb{E}[\mathbf{s}\mathbf{s}^H] = \sigma_s^2\mathbf{I}_{Nu}$, in which σ_s^2 is its variance. The term $\mathbf{R}_{ff} = \mathbb{E}[\mathbf{f}\mathbf{f}^H]$ stands for the autocorrelation of the distortion vector \mathbf{f} . Next, we can notice that in full resolution, since there is no quantization and its associated distortion, (8) turns into

$$\mathbf{s}_q = \mathbf{P}\mathbf{s}, \quad (78)$$

where we make $\mathbf{T}_{n,n} = \mathbf{I}_{Nb \times Nb}$, i.e., $\delta = 1$ in (69), and assume that $\mathbf{f} = \mathbf{0}_{Nb}$. Now, we calculate the autocorrelation of the full resolution precoded symbol vector (78) as follows:

$$\begin{aligned} \mathbf{R}_{sqsq} &= \mathbb{E}[(\mathbf{P}\mathbf{s})(\mathbf{P}\mathbf{s})^H] \\ &= \mathbb{E}[\mathbf{P}\mathbf{s}\mathbf{s}^H\mathbf{P}^H] \\ &= \sigma_s^2\mathbf{M}\mathbf{P}^H, \end{aligned} \quad (79)$$

By equating (77) and (79), we can obtain the expression of the autocorrelation of the distortion vector:

$$\begin{aligned}\delta^2 \sigma_s^2 \mathbf{P}\mathbf{P}^H + \mathbf{R}_{ff} &= \sigma_s^2 \mathbf{P}\mathbf{P}^H \\ \therefore \mathbf{R}_{ff} &= (1 - \delta^2) \sigma_s^2 \mathbf{P}\mathbf{P}^H\end{aligned}\quad (80)$$

We can then compute the autocorrelation matrix of (75):

$$\begin{aligned}\mathbf{R}_{yy} &= \mathbb{E}[\mathbf{y}\mathbf{y}^H] \\ &= (\mathbf{H}\mathbf{T}\mathbf{P}) \mathbf{R}_{ss} (\mathbf{H}\mathbf{T}\mathbf{P})^H \\ &\quad + \mathbf{H} \mathbf{R}_{ff} \mathbf{H}^H + \mathbf{R}_{nn},\end{aligned}\quad (81)$$

where $\mathbf{R}_{ss} = \mathbb{E}[\mathbf{s}\mathbf{s}^H]$, $\mathbf{R}_{ff} = \mathbb{E}[\mathbf{f}\mathbf{f}^H]$ and $\mathbf{R}_{nn} = \mathbb{E}[\mathbf{n}\mathbf{n}^H]$ are the autocorrelation matrices of the signal, the distortion and the noise vectors, respectively. Similar procedure applied to the distortion-plus-noise vector (76), considering the conditions above, yields

$$\mathbf{R}_{\tilde{\mathbf{n}}\tilde{\mathbf{n}}} = \mathbb{E}[\tilde{\mathbf{n}}\tilde{\mathbf{n}}^H] = \mathbf{H}\mathbf{R}_{ff}\mathbf{H}^H + \mathbf{R}_{nn},\quad (82)$$

From the principles of information theory [53] and the capacity of a frequency flat deterministic MIMO channel [29], we can bound the achievable rate in bits per channel use at which information can be sent with arbitrarily low probability of error by the mutual information of a Gaussian channel, i.e.

$$\begin{aligned}C &\leq I(\mathbf{s}, \mathbf{y}) = \Upsilon(\mathbf{y}) - \Upsilon(\mathbf{y}|\mathbf{s}) \\ &= \Upsilon(\mathbf{y}) - \Upsilon(\tilde{\mathbf{n}}) \\ &= \log_2 [\det(\pi e \mathbf{R}_{yy})] - \log_2 [\det(\pi e \mathbf{R}_{\tilde{\mathbf{n}}\tilde{\mathbf{n}}})] \\ &= \log_2 [\det(\mathbf{R}_{yy})] - \log_2 [\det(\mathbf{R}_{\tilde{\mathbf{n}}\tilde{\mathbf{n}}})] \\ &= \log_2 [\det(\mathbf{R}_{yy} \mathbf{R}_{\tilde{\mathbf{n}}\tilde{\mathbf{n}}}^{-1})]\end{aligned}\quad (83)$$

where $\Upsilon(\mathbf{y})$ and $\Upsilon(\mathbf{y}|\mathbf{s}_q)$ are the differential and the conditional differential entropies of \mathbf{y} , respectively. By combining (81) and (82) with (83), we have:

$$\begin{aligned}C &\leq \log_2 \left\{ \det \left[\left((\mathbf{H}\mathbf{T}\mathbf{P}) \mathbf{R}_{ss} (\mathbf{H}\mathbf{T}\mathbf{P})^H \right) \right. \right. \\ &\quad \left. \left. (\mathbf{H}\mathbf{R}_{ff}\mathbf{H}^H + \mathbf{R}_{nn})^{-1} + \mathbf{I}_{N_u} \right] \right\}\end{aligned}\quad (84)$$

In Section II, we have defined the total power as $P = SNR N_0$. From the definition of the noise vector, also in that Section, we can express its covariance matrix as $\mathbf{R}_{nn} = N_0 \mathbf{I}_{N_u}$. Combining the two previously

mentioned expressions, we obtain

$$\mathbf{R}_{nn} = \frac{P}{SNR} \mathbf{I}_{N_u} \quad (85)$$

Recalling from Section II that $\mathbf{R}_{ss} \approx \mathbf{I}_{N_u}$ and assuming that the total power is given by $P = \text{trace}(\mathbf{R}_{ss}) = N_u$, (85) turns into

$$\mathbf{R}_{nn} = \frac{N_u}{SNR} \mathbf{I}_{N_u} \quad (86)$$

By combining (84), (80) (69) and the expression of \mathbf{R}_{ss} previously mentioned with (86), followed by algebraic manipulation, we obtain

$$C = \log_2 \left\{ \det \left[\mathbf{I}_{N_u} + \delta^2 \frac{SNR}{N_u} (\mathbf{HP})(\mathbf{HP})^H \right. \right. \\ \left. \left. \left((1 - \delta^2) \frac{SNR}{N_u} (\mathbf{HP})(\mathbf{HP})^H + \mathbf{I}_{N_u} \right)^{-1} \right] \right\} \quad \square \quad (87)$$

REFERENCES

- [1] Rusek, F. et al: 'Scaling up MIMO: Opportunities and challenges with very large large arrays', *IEEE Signal Process. Mag.*, **30**, (1), pp.40-60, Jan. 2013.
- [2] Larsson, E. G., Edfors, O., Tufvesson, F., Marzetta, T. L.: 'Massive MIMO for next generation wireless systems', *IEEE Commun. Mag.*, **52**, (2), pp.186-195, Feb. 2014.
- [3] Lu, L., Li, G.Y., Swindlehurst, A. L., Ashikhmin, A., Zhang, R.: 'An overview of massive MIMO: Benefits and challenges', *IEEE J. Sel. Topics Signal Process.*, **8**, (5), pp.742-758, Oct. 2014.
- [4] Sarajlic, M., Liu, L., Swindlehurst, A. L., Edfors, O., 'An overview of massive MIMO: Benefits and challenges', Proc. 50th Asilomar Conference on Signals, Systems and Computers, pp. 1-6, 2016.
- [5] de Lamare, R. C., "Massive MIMO systems: Signal processing challenges and future trends," in URSI Radio Science Bulletin, vol. 2013, no. 347, pp. 8-20, Dec. 2013.
- [6] Zhang, W., et al., "Large-Scale Antenna Systems With UL/DL Hardware Mismatch: Achievable Rates Analysis and Calibration," *IEEE Transactions on Communications*, vol. 63, no. 4, pp. 1216-1229, April 2015.
- [7] Bussgang, J. J., 'Crosscorrelation functions of amplitude-distorted Gaussian signals', Res. Lab. Electron., Cambridge, MA, USA, Tech. Rep. 216, Mar. 1952.
- [8] Jacobsson, S., Durisi, G., Coldrey, M., Goldstein, T., Studer, C., 'Quantized precoding for massive MU-MIMO', *IEEE Trans. on Communications*, **65**, (11), Nov. 2017.
- [9] Jacobsson, S., Durisi, G., Coldrey, M., Studer, C., 'Linear Precoding With Low-Resolution DACs for Massive MU-MIMO-OFDM Downlink', *IEEE Transactions on Wireless Communications*, **18**, (3), Mar. 2019.
- [10] Jacobsson, S., Durisi, G., Coldrey, M., Gustavsson, U., Studer, C., 'Throughput Analysis of Massive MIMO Uplink With Low-Resolution ADCs', *IEEE Transactions on Wireless Communications*, **16**, (6), Jun. 2017.
- [11] Tsinos, C. G., Kalantari, A., Chatzinotas, S. and Ottersten, B., "Symbol-Level Precoding with Low Resolution DACs for Large-Scale Array MU-MIMO Systems," *2018 IEEE SPAWC*, Kalamata, 2018, pp. 1-5.
- [12] Rowe, H., 'Memoryless nonlinearities with Gaussian inputs: Elementary results', *Bell System Technical Journal*, **61**, (7), pp.1519-1525, Sep. 1982.
- [13] Landau, L. T. N., Lamare, R. C., 'Branch-and-Bound Precoding for Multiuser MIMO Systems With 1-Bit Quantization', *IEEE Wireless Communications Letters*, **6**,(6), Dec. 2017
- [14] Pinto, S. F. B., Lamare, R.C., 'Coarse Quantization-Aware Block Diagonalization Algorithms for Multiple-Antenna Systems with Low-Resolution Signals', 24th International ITG Workshop on Smart Antennas, pp.1-6, Hamburg, Germany, Feb.2020.
- [15] Miller, K.S., 'On the Inverse of the Sum of Matrices', *Mathematics Magazine*, Mar., 1981, Vol. 54, No. 2 (Mar., 1981), pp. 67-72.
- [16] Seber, G. A. F., 'A Matrix Handbook for Statisticians', Wiley, 2008.

- [17] Harville, D.A., 'Matrix Algebra From a Statistician's Perspective', Springer 1997.
- [18] Telatar, I. E., 'Capacity of Multi-Antenna Gaussian Channels', Rm.2C-174, Lucent Technologies, Bell Laboratories, 1999.
- [19] Anton, H., Busby, R. C., 'Contemporary Linear Algebra', Wiley, 2002.
- [20] Withers, Christopher S., Nadarajah, S., 'log det A = tr log A', International Journal of Mathematical Education in Science and Technology, Vol.41, No 8 , Aug.,2010, pp.1121-1124.
- [21] Mezghani, A., Ghiat, R., Nossek, J. A., 'Transmit processing with low resolution D/A-converters', 16th IEEE International Conference on Electronics, Circuits and Systems, pp.1-4, 2009.
- [22] Joham, M., Utschick, W., Nossek, J. A., 'Linear transmit Processing in MIMO Communications Systems', *IEEE Trans. on Signal Processing*, vol. 53, no. 8, pp. 2700-2712, Aug. 2005.
- [23] Spencer, Q. H. , Swindlehurst, A. L. and Haardt, M., "Zero-forcing methods for downlink spatial multiplexing in multiuser MIMO channels," in IEEE Transactions on Signal Processing, vol. 52, no. 2, pp. 461-471, Feb. 2004.
- [24] Sung, H., Lee, S., Lee, I., 'Generalized Channel Inversion Methods for Multiuser MIMO Systems', *IEEE Transactions on Communications*, **57**, (11), Nov. 2009.
- [25] Stankovic, V., Haardt, M., 'Generalized Design of Multi-User MIMO Precoding Matrices', *IEEE Transactions on Wireless Communications*, **7**, (3), Mar. 2008.
- [26] Zu, K. and de Lamare R. C., 'Low-Complexity Lattice Reduction-Aided Regularized Block Diagonalization for MU-MIMO Systems,' *IEEE Communications Letters*, vol. 16, no. 6, pp. 925-928, June 2012.
- [27] Zu, K., Lamare, R. C., and Haardt, M., 'Generalized Design of Low-Complexity Block Diagonalization Type Precoding Algorithms for Multiuser MIMO Systems', *IEEE Transactions on Communications*, **61**, (10), Oct. 2013.
- [28] Zhang, W. et al., 'Widely Linear Precoding for Large-Scale MIMO with IQI: Algorithms and Performance Analysis,' *IEEE Transactions on Wireless Communications*, vol. 16, no. 5, pp. 3298-3312, May 2017.
- [29] Paulraj, A., Nabar, R., Gore, D., 'Introduction to Space-Time Wireless Communications', Cambridge University Press, 2003.
- [30] S. F. B. Pinto and R. C. de Lamare, "Block Diagonalization Precoding and Power Allocation for Multiple-Antenna Systems with Coarsely Quantized Signals", *IEEE Transactions on Communications*, 2021.
- [31] L. T. N. Landau, M. Dörpinghaus, R. C. de Lamare and G. P. Fettweis, "Achievable Rate With 1-Bit Quantization and Oversampling Using Continuous Phase Modulation-Based Sequences," in IEEE Transactions on Wireless Communications, vol. 17, no. 10, pp. 7080-7095, Oct. 2018.
- [32] Z. Shao, L. T. N. Landau and R. C. de Lamare, "Dynamic Oversampling for 1-Bit ADCs in Large-Scale Multiple-Antenna Systems," in IEEE Transactions on Communications, vol. 69, no. 5, pp. 3423-3435, May 2021
- [33] W. Zhang et al., "Large-Scale Antenna Systems With UL/DL Hardware Mismatch: Achievable Rates Analysis and Calibration," in IEEE Transactions on Communications, vol. 63, no. 4, pp. 1216-1229, April 2015.
- [34] Y. Cai, R. C. de Lamare and R. Fa, "Switched Interleaving Techniques with Limited Feedback for Interference Mitigation in DS-CDMA Systems," in IEEE Transactions on Communications, vol. 59, no. 7, pp. 1946-1956, July 2011
- [35] Y. Cai, R. C. de Lamare and D. Le Ruyet, "Transmit Processing Techniques Based on Switched Interleaving and Limited Feedback for Interference Mitigation in Multiantenna MC-CDMA Systems," in IEEE Transactions on Vehicular Technology, vol. 60, no. 4, pp. 1559-1570, May 2011
- [36] Y. Cai, R. C. de Lamare, L. Yang and M. Zhao, "Robust MMSE Precoding Based on Switched Relaying and Side Information for Multiuser MIMO Relay Systems," in IEEE Transactions on Vehicular Technology, vol. 64, no. 12, pp. 5677-5687, Dec. 2015.
- [37] X. Lu and R. C. de Lamare, "Opportunistic Relaying and Jamming Based on Secrecy-Rate Maximization for Multiuser Buffer-Aided Relay Systems," in IEEE Transactions on Vehicular Technology, vol. 69, no. 12, pp. 15269-15283, Dec. 2020
- [38] V. M. T. Palhares, A. R. Flores and R. C. de Lamare, "Robust MMSE Precoding and Power Allocation for Cell-Free Massive MIMO Systems," in IEEE Transactions on Vehicular Technology, vol. 70, no. 5, pp. 5115-5120, May 2021
- [39] A. R. Flores, R. C. de Lamare and B. Clerckx, "Linear Precoding and Stream Combining for Rate Splitting in Multiuser MIMO Systems," in IEEE Communications Letters, vol. 24, no. 4, pp. 890-894, April 2020,
- [40] K. Zu, R. C. de Lamare and M. Haardt, "Multi-Branch Tomlinson-Harashima Precoding Design for MU-MIMO Systems: Theory and Algorithms," in IEEE Transactions on Communications, vol. 62, no. 3, pp. 939-951, March 2014.
- [41] L. Zhang, Y. Cai, R. C. de Lamare and M. Zhao, "Robust Multibranch Tomlinson-Harashima Precoding Design in Amplify-and-Forward MIMO Relay Systems," in IEEE Transactions on Communications, vol. 62, no. 10, pp. 3476-3490, Oct. 2014,
- [42] S. D. Somasundaram, N. H. Parsons, P. Li and R. C. de Lamare, "Reduced-dimension robust capon beamforming using Krylov-subspace techniques," in IEEE Transactions on Aerospace and Electronic Systems, vol. 51, no. 1, pp. 270-289, January 2015.
- [43] N. Song, W. U. Alokozai, R. C. de Lamare and M. Haardt, "Adaptive Widely Linear Reduced-Rank Beamforming Based on Joint Iterative Optimization," in IEEE Signal Processing Letters, vol. 21, no. 3, pp. 265-269, March 2014

- [44] H. Ruan and R. C. de Lamare, "Robust Adaptive Beamforming Using a Low-Complexity Shrinkage-Based Mismatch Estimation Algorithm," in *IEEE Signal Processing Letters*, vol. 21, no. 1, pp. 60-64, Jan. 2014
- [45] H. Ruan and R. C. de Lamare, "Robust Adaptive Beamforming Based on Low-Rank and Cross-Correlation Techniques," in *IEEE Transactions on Signal Processing*, vol. 64, no. 15, pp. 3919-3932, 1 Aug.1, 2016
- [46] H. Ruan and R. C. de Lamare, "Distributed Robust Beamforming Based on Low-Rank and Cross-Correlation Techniques: Design and Analysis," in *IEEE Transactions on Signal Processing*, vol. 67, no. 24, pp. 6411-6423, 15 Dec.15, 2019
- [47] A. R. Flores, R. C. De Lamare and B. Clerckx, "Tomlinson-Harashima Precoded Rate-Splitting With Stream Combiners for MU-MIMO Systems," in *IEEE Transactions on Communications*, vol. 69, no. 6, pp. 3833-3845, June 2021.
- [48] T. Peng, R. C. de Lamare and A. Schmeink, "Adaptive Distributed Space-Time Coding Based on Adjustable Code Matrices for Cooperative MIMO Relaying Systems," in *IEEE Transactions on Communications*, vol. 61, no. 7, pp. 2692-2703, July 2013
- [49] J. Gu, R. C. de Lamare and M. Huemer, "Buffer-Aided Physical-Layer Network Coding With Optimal Linear Code Designs for Cooperative Networks," in *IEEE Transactions on Communications*, vol. 66, no. 6, pp. 2560-2575, June 2018
- [50] Y. Jiang et al., "Joint Power and Bandwidth Allocation for Energy-Efficient Heterogeneous Cellular Networks," in *IEEE Transactions on Communications*, vol. 67, no. 9, pp. 6168-6178, Sept. 2019.
- [51] Naber, J., Singh, H. , Sadler, R., Milan, J., 'A low-power, high-speed 4-bit GAAS ADC and 5-bit DAC', Proc. 11th Annu. Gallium Arsenide Integr. Circuit Symp., San Diego, CA, USA, pp.333-336, Oct. 1989.
- [52] Orhan, O., Erkip, E., Rangan, S., 'Low power analog-to-digital converter in millimeter wave systems: Impact of resolution and bandwidth on performance', Information theory and Applications Workshop, pp. 191-198, Feb.2015.
- [53] Cover, T.H., Thomas, J. A., 'Elements of Information Theory', Second Edition, Wiley, 2006.
- [54] Wei Yu, Wonjong Rhee, S. Boyd and J. M. Cioffi, 'Iterative water-filling for Gaussian vector multiple-access channels,' *IEEE Transactions on Information Theory*, vol. 50, no. 1, pp. 145-152, Jan. 2004.
- [55] Palomar, D.P., Fonollosa, J. R., 'Practical Algorithms for a Family of Waterfilling Solutions', *IEEE Transactions on Signal Processing*, **53**, (2), Feb. 2005.
- [56] Khan, M.H.A., Cho, K.M., Lee, M.H. et al. , 'A simple block diagonal precoding for multi-user MIMO broadcast channels', *J Wireless Com Network*, 95, 2014.
- [57] Bussgang, J.J., 'Crosscorrelation functions of amplitude-distorted Gaussian signals', Res. Lab. Elec., Cambridge, MA, USA, Tech. Rep. 216, Mar. 1952.
- [58] Loyka, S. L., 'Channel capacity of MIMO architecture using the exponential correlation matrix', *IEEE Communications Letters*, vol.5, no. 9, pp. 369-371, Sept. 2001.
- [59] Windpassinger, C., 'Detection and precoding for multiple input multiple output channels', Ph.D. dissertation, Univ. Erlangen-Nurnberg, Erlangen, Germany, 2004.
- [60] Z. Shao, L. T. N. Landau and R. C. De Lamare, "Channel Estimation for Large-Scale Multiple-Antenna Systems Using 1-Bit ADCs and Oversampling," in *IEEE Access*, vol. 8, pp. 85243-85256, 2020.
- [61] R. C. de Lamare and R. Sampaio-Neto, "Adaptive Reduced-Rank Processing Based on Joint and Iterative Interpolation, Decimation, and Filtering," in *IEEE Transactions on Signal Processing*, vol. 57, no. 7, pp. 2503-2514, July 2009.
- [62] R. C. de Lamare and R. Sampaio-Neto, "Reduced-Rank Adaptive Filtering Based on Joint Iterative Optimization of Adaptive Filters," in *IEEE Signal Processing Letters*, vol. 14, no. 12, pp. 980-983, Dec. 2007
- [63] Y. Cai, R. C. de Lamare, B. Champagne, B. Qin and M. Zhao, "Adaptive Reduced-Rank Receive Processing Based on Minimum Symbol-Error-Rate Criterion for Large-Scale Multiple-Antenna Systems," in *IEEE Transactions on Communications*, vol. 63, no. 11, pp. 4185-4201, Nov. 2015.
- [64] R. C. De Lamare and R. Sampaio-Neto, "Minimum Mean-Squared Error Iterative Successive Parallel Arbitrated Decision Feedback Detectors for DS-CDMA Systems," in *IEEE Transactions on Communications*, vol. 56, no. 5, pp. 778-789, May 2008.
- [65] P. Li, R. C. de Lamare and R. Fa, "Multiple Feedback Successive Interference Cancellation Detection for Multiuser MIMO Systems," in *IEEE Transactions on Wireless Communications*, vol. 10, no. 8, pp. 2434-2439, August 2011.
- [66] R. C. de Lamare, "Adaptive and Iterative Multi-Branch MMSE Decision Feedback Detection Algorithms for Multi-Antenna Systems," in *IEEE Transactions on Wireless Communications*, vol. 12, no. 10, pp. 5294-5308, October 2013.
- [67] A. G. D. Uchoa, C. T. Healy and R. C. de Lamare, "Iterative Detection and Decoding Algorithms for MIMO Systems in Block-Fading Channels Using LDPC Codes," in *IEEE Transactions on Vehicular Technology*, vol. 65, no. 4, pp. 2735-2741, April 2016.
- [68] Z. Shao, R. C. de Lamare and L. T. N. Landau, "Iterative Detection and Decoding for Large-Scale Multiple-Antenna Systems With 1-Bit ADCs," in *IEEE Wireless Communications Letters*, vol. 7, no. 3, pp. 476-479, June 2018.
- [69] A. Danaee, R. C. de Lamare and V. H. Nascimento, "Energy-Efficient Distributed Learning With Coarsely Quantized Signals," in *IEEE Signal Processing Letters*, vol. 28, pp. 329-333, 2021.
- [70] R. B. Di Renna and R. C. de Lamare, "Iterative List Detection and Decoding for Massive Machine-Type Communications," in *IEEE Transactions on Communications*, vol. 68, no. 10, pp. 6276-6288, Oct. 2020